Supporting Information Text S1, Figs S1-S3; Tables S1-S6

Belonging to the paper De Vos, Hughes, Schneeweiss, Moore & Conti "*Heterostyly accelerates diversification via reduced extinction in primroses*" Proceedings of the Royal Society B: Biological Sciences

Text S1

Sampling strategy—Comparative methods assume that extant species are either completely or randomly sampled. Accordingly, we sought to minimize the effects of incomplete sampling on our comparative inferences by including species from all genera and sections of Primulaceae in proportion both to the total number of species in each taxon and to the number of species with heterostylous and non-heterostylous flower morphologies (Table S4). Traditional taxonomic delimitation of groups below the genus level (in subgenera and sections) is based on morphological characters that often do not reflect phylogenetic affinities of species (e.g. [1-3]). Hence, by including species from all genera and sections, morphological diversity is well represented, although we cannot assign unsampled species to any specific tips in downstream comparative analyses. For *Primula,* we generally sampled one accession from species that are known to be monomorphic for breeding system (*i.e.*, with exclusively heterostylous or non-heterostylous flowers), and sampled two accessions for species that are polymorphic for breeding system (e.g., *Primula cuneifolia*). Information on species numbers and breeding systems was drawn primarily from [1-6] (see Tables S4, S6 for details). In total, our dataset included 265 taxa, representing 36–38% of extant diversity (the exact percentage depends on the taxonomic authority followed, see Note 2 in Table S4), the most complete sampling of Primulaceae in a phylogenetic study to date.

DNA amplification, sequencing, and sequence alignment—Total genomic DNA was extracted from silica-dried leaves as described in [1,2]. We amplified and sequenced loci of the chloroplast genome that allowed us to combine our newly generated data with existing sequence data for /Primula [2,3], /Androsace [1] and /Soldanella [2]. DNA sequences from the tRNA-Leu (*trn*L) intron and the *trn*L-*trn*F intergenic spacer (hereafter *trn*L-F), and the maturase K gene (hereafter *mat*K) were obtained for all taxa, those from the intron of the ribosomal protein L16 (hereafter *rpl*16) for 89% of taxa. A total of 210 new DNA sequences were generated for 73 species as part of this study and included in a matrix with 820 additional sequences retrieved from GenBank (Table S6). PCR amplification followed [7], but with 32 cycles (or up to 36 if yields were low) of 30 s at 95º, 60 s at 52º, and 100 s at 72º, followed by a final extension period of 10 min at 72º, using the following primers: *trn*L-F: trnc, trnd, trne, trnf [8]; *mat*K: MatK1F, MatK3F, MatK1R [9], and the newly designed sequencing primers MatK3Frc (5'-ATG CAA AGA AGA GGC ATC TT-3', i.e., the reverse complement of primer MatK3F), MatK4F (5'-TTT CTT GTG CTA GAA CTT TGG-3', which anneals between MatK3F and MatK1R); *rpl*16: F71 [10], R1516 [11]. PCR products were cleaned using Qiaquick spin columns (Qiagen AG, Basel, Switzerland) and cycle-sequencing was performed using BigDye Terminator v.3.1 (Applied Biosystems, Foster City CA, USA), using the manufacturer's protocols. Sequencing products were purified with Sephadex G-50 fine grade (GE Healthcare, Glattbrugg, Switzerland), and loaded on a 3130xl DNA Analyzer (Applied Biosystems, Zug, Switzerland). Electropherograms were checked and assembled into consensus sequences using the Staden Package v.1.6.0 (http://staden.sourceforge.net/). Alignments for each region were obtained using MUSCLE [12] (with manual corrections when sequences contained long gaps; these tended to be erroneously broken up into several smaller gaps), and sites with >50% missing data were excluded from the analysis, which removed all ambiguously aligned hyper-variable regions. Our final dataset contained 3351 sites for 265 taxa and contained 5.9% gaps or missing data and is available under TreeBASE reference TB2:S14824.

Phylogeny and divergence time estimation—We estimated divergence times from the sampled sequences using a Bayesian relaxed-molecular clock approach. Relaxed-clock models are comprised of three main components: (1) A *site model* describes how the sequence data evolved over the tree with branch durations; (2) a *branch-rate prior model* specifies how substitution rates are distributed among branches of the tree; and (3) a *node-age prior model* is also required to specify the distribution of branching times in the tree. We used a mixed-model selection approach [60] to assess the fit of candidate site models to the primrose sequence data. Four candidate mixed

models specified alternative "data partitions" (where subsets of sites were variously assigned to separate substitution models) in an effort to accommodate process heterogeneity among gene regions. The fit of substitution models to each of the data partitions comprising each of the mixed models was assessed by means of ΔAIC scores [14] calculated using Modeltest v.3.7 [16]. We then approximated the joint posterior probability for each of the four candidate mixed models using the MCMC algorithms implemented in MrBayes 3.1.2 [15]: each independent chain was run for 15 million cycles using default priors. For all analyses involving MCMC, we assessed MCMC performance by examining all parameters (including the topology) using Tracer [13] and AWTY [18]. The sampled likelihoods from these analyses were then used to estimate the marginal likelihood of each candidate partition scheme using the harmonic-mean estimator implemented in Tracer v.1.5 [13]. Finally, the relative fit of the competing mixed models was assessed using Bayes factors [14]. This identified a mixed model with an independent GTR+ Γ substitution model assigned to each of five separate data partitions; *i.e.*, the *trn*L + *trn*L-F regions, the *rpl*16 region, and the three codon positions for the *mat*K gene. The resulting site model was assumed for subsequent analyses.

We assessed the fit of the primrose sequence data to two prior branch-rate models, which describe how substitution rates vary among branches: the uncorrelated lognormal (UCLN) and uncorrelated exponential (UCEXP) models. Specifically, we approximated the joint posterior probability under each branch-rate model using the MCMC algorithms implemented in BEAST v.1.6.2 [13]. Each relaxed-clock model comprised the previously selected site model and assumed a general birth-death node-age prior model (using default priors densities for all parameters). The three main clades /Primula, /Soldanella, /Androsace, which are strongly supported by the MrBayes analyses with optimal partitioning scheme (posterior probability 1.0; Fig. S1A), were constrained to be monophyletic. For each branch-rate model, we ran six independent MCMC simulations for 50 million cycles, thinning samples of trees every 2500th cycle and continuous parameter values every 1000th cycle. As previously, the relative fit of the two candidate relaxed-clock models to the primrose sequence data was then assessed by calculating Bayes factors based on estimates of the marginal likelihood for each relaxed-clock model. This procedure revealed that relaxed-clock models using both the UCLN and UCEXP branch-rate prior models provide a similar fit to the primrose data. We accommodated uncertainty in the choice of relaxed-clock model by using both models in subsequent analyses.

Estimates of absolute divergence times in primroses were summarized as maximum clade credibility (MCC) trees with median node heights (Figs S1B,C). Inferences under each of the models were based on combined stationary samples from independent chains, which provided adequate sampling for all parameters

according to estimated effective sample sizes (ESS). Phylogenetic analyses were performed on the CIPRES science gateway (http://www.phylo.org) or locally.

Calibration—Estimating absolute divergence times requires the inclusion of external information on the age of one or more nodes. We used a combination of direct fossil evidence and "legacy-calibration" estimates to infer the absolute divergence times in primroses. The fossil record of Primulaceae is too sparse to provide multiple, reliable calibrations within Primulaceae (see also [1,19,20]). Miocene seeds assigned to *Androsace* [21-23] are problematic for calibration, because they lack clear diagnostic morphological synapomorphies with extant taxa. However, fossil seeds of *Primula riosiae*, also from the Miocene [24], can be used to assign a minimum age of 15.97 Ma (the early-mid Miocene boundary) to the split between /Primula and /Soldanella. This direct fossil evidence was augmented by a legacy calibration for the root of the tree; this approach relies on age estimates based on a more inclusive analysis. The use of legacy calibrations has been justifiably criticized for failing to appropriately accommodate uncertainty in the age estimates [25]. We addressed this concern by specifying a prior probability density for the legacy calibration that captures the uncertainty in the estimated age of the root node.

To this end, we performed a completely separate series of divergence-time analyses from a taxonomically more inclusive sample of six plastid gene regions (from *mat*K, *ndh*F, *rbc*L coding regions and *trn*L, *rps*16, *trn*V non-coding gene regions) sourced from GenBank. The resulting data matrix comprised 8446 aligned sites and 21 species of Ericales (which include Primulaceae), with 4.7% missing data (Table S5). Sequence alignment, model specification and parameter estimation proceeded as described above for Primulaceae, unless otherwise stated. Fossils of *Eurya* (Santonian; 85.8±0.7 Ma to 83.5±0.7 Ma) and *Saurauia* (Turonian; 93.6±0.8 Ma to ~88.6 Ma) [26] were applied as lognormal priors to constrain the divergence between Actinidiaceae and Roridulaceae and between *Pentaphylax* and *Ternstroemia* (Pentaphylacaceae), respectively (see also [27]). Specifically, we specified lognormal calibration prior densities with offsets of 82.8 and 88.6 (representing minimum age of respective geological strata), means of 1.85 and 2.50, and standard deviations of 0.965 and 0.558, respectively. A maximum age of 125 Ma (Barremian-Aptian boundary) was assigned to the root, corresponding to the oldest pollen record for Eudicots [28,29]. Stratigraphic age estimates followed the International Commission of Stratigraphy, September 2010 (http://www.stratigraphy.org).

As in the primrose dataset, divergence-time analyses revealed that both the UCLN and UCEXP relaxed-clock models have a similar fit to the Ericales dataset: the marginal log-likelihood estimates were -42055.041 ± 0.223 and -42055.195 ± 0.238, for the UCLN and UCEXP branch-rate prior models, respectively. However, the

inferred age of the basal divergence in primroses (i.e., the *Primula-Androsace* divergence) under these two models differed substantially: UCLN, mean age 41.88 Ma, 95% highest posterior density (HPD) 24.23–60.34 Ma; UCEXP, mean age 36.37 Ma, 95% HPD 18.79–55.07 Ma. We therefore specified a model-averaged calibration prior density for the root of the primroses based on age estimates from both the UCLN and UCEXP relaxed-clock model. Specifically, we constructed a composite marginal distribution of dated trees from posterior samples under both relaxed-clock models. The mean age of the primrose root node in the composite-marginal distribution had a mean of 38.82 MY, 95% HPD 21.09–58.90 MY. We specified a calibration prior density for the primrose root node using a Gaussian probability density with mean 39.99645 and standard deviation 11.492, which thus contains 95% of the probability density within the interval 21.09–58.90.

Character history—Heterostyly occurs in ca. 85% of all species in /Primula (Table S4). In this clade, stigmas and anthers are positioned typically in the middle of the corolla tubes of short-styled and long-styled morphs, respectively, whereas the alternate sexual organs are placed at the mouth of the corolla tubes in the respective morphs (distyly; Fig. 1 main text). *Hottonia palustris* (/Soldanella) and *Androsace vitaliana* (/Androsace) are also distylous, but in a form is distinct from that typical of /Primula. Specifically, the short-style morph of *Hottonia palustris* has long filaments that are largely free, with the anthers exerted above the flowers [30], while *Androsace vitaliana* has strong stylar, but weak staminal dimorphism ([31]; pers. obs.). The vast majority of heterostylous species are strongly self-incompatible [4], while non-heterostylous species show full fertility after self-fertilization; self-incompatibility has not been documented for any non-heterostylous Primulaceae species (e.g., [4,30,32,33]). Because species that lack heterostyly may have flowers of various shapes and sizes, we refrain from using the term “homostylous”, which typically refers to florally monomorphic species secondarily derived from heterostylous ancestors [2] with anthers and stigmatic surfaces in close proximity within flowers. Flowers in the three main clades appear relatively similar, irrespective of the presence of heterostyly, usually with narrow corolla tubes (exceptions occur e.g. in genera *Soldanella* in /Soldanella and *Dodecatheon* and *Cortusa* in /Primula). For instance, several species of *Androsace* and *Primula* have been transferred between the genera throughout their taxonomic history, cf. *Androsace* sect. *Pseudoprimula*. The overall similarity justifies our relatively simple binary scoring scheme.

Presence of heterostyly was scored as a binary trait, under four different character-coding schemes. Three schemes were designed to accommodate ten species for which some but not all populations have been reported to be heterostylous, or for which available information on heterostyly is inconclusive. Under scheme 1, these species

were scored as heterostylous; under scheme 2, they were scored according to the predominant breeding system for the species based on [6] and taxonomic descriptions (explained in notes of Table S6); under scheme 3, they were scored as non-heterostylous. Under scheme 4, *Androsace vitaliana* and *Hottonia palustris* were scored as non-heterostylous, because of their atypical floral polymorphism, whilst employing scheme 2 for all other species. Comparing the results obtained using the four character coding schemes allowed for a more rigorous assessment of the effect of polymorphic species on ancestral-state estimation compared to employing a character coding scheme that includes multi-state scoring.

Based on the four character-coding schemes, we estimated ancestral states at five key internal nodes (a–e, Fig. 2 main text) with Bayesian methods (using BayesTraits v.1.0) and maximum-likelihood methods (using the function asr.marginal in R-package diversitree [41]). Maximum-likelihood estimation was performed under the unconstrained BiSSE model, which avoids potential bias in ancestral-states estimates associated with potential influence of traits on speciation and/or extinction rates [41]. The close correspondence of ancestral-state estimates under these approaches provides strong support for the inferred history of heterostyly in Primulaceae.

All analyses were performed on a sample of 1000 trees from the posterior distribution under both dating analyses. Bayesian (BI) and maximum-likelihood analyses (ML) employed a model with separate parameters for forward and reverse rates (i.e., q_{01} and q_{10}), which provided a better fit to the data better than a symmetrical model in initial runs. ML analyses calculated the proportion of likelihood associated with selected backbone nodes being heterostylous or not, averaged across 1,000 trees from the posterior distributions of trees to reflect phylogenetic uncertainty. BI analyses inferred the posterior probability density for the five nodes of interest to be heterostylous, while averaging across trees during MCMC. To facilitate comparison of ML and BI results, median probabilities ± interquartile ranges are reported in Table S1. Statistical support for heterostyly as the ancestral state was determined by constraining each of the five nodes of interest in turn to be either heterostylous or non-heterostylous and performing an MCMC analysis. This way, we inferred the marginal likelihood associated with each state at nodes of interest (using the harmonic mean estimator implemented in BayesTraits) and calculated the BayesFactor to infer if either state was significantly supported. MCMC chains were sampled every $1{,}000^{th}$ generation for 10 million generations, after a burnin phase of 500,000 generations. To achieve adequate MCMC performance, we adjusted the proposal window by setting the rate deviation to 0.05, after an initial set of runs, and employed exponential priors with mean 1 for rate parameters. We obtained qualitatively identical results using uniform priors or exponential hyper-priors.

Detection of diversification rate shifts—We used MEDUSA (implemented in the geiger 1.99-3.1 package [36] in R v.3.0.2) to identify shifts in diversification rates along branches of the tree where ancestral-state estimates inferred the origin of heterostyly. MEDUSA analyses were performed on MCC trees estimated under each of the two relaxed-clock models. Because MEDUSA has a high Type-I error rate (BRM, unpublished data), we specified a conservative threshold (ΔAICc cut-off of 4) to assess the improvement in fit of increasingly complex diversification-rate models. We explored the impact of phylogenetic uncertainty on the inferred diversification-rate shifts by performing MEDUSA analyses on 100 samples from the posterior distribution of trees. Because estimates of diversification-rate shifts using MEDUSA is sensitive to arbitrarily specified ΔAICc thresholds ([61], BRM, unpublished data), we independently identified the location of diversification-rate shifts using SymmeTREE v.1.1 [37]. SymmeTREE uses Monte Carlo simulation to generate a null distribution of the likelihood-ratio test statistic used to assess diversification-rate shifts at each branch, which guarantees that the Type I error rate is no greater than the specified critical value, $\alpha = 0.05$ [37]. SymmeTREE analyses were performed on the 50% majority rule consensus trees summarizing the marginal posterior probability distribution of trees estimated under each of the two relaxed-clock models.

MEDUSA and SymmeTREE are both agnostic to the presence or location of diversification-rate shifts. That is, these methods are primarily used without *a priori* hypotheses regarding the location of putative diversification-rate shifts. We complemented results based on these two exploratory approaches with a Bayesian hypothesis-testing approach implemented in BayesRate v.1.3.41 [38]. This requires specifying partitions of the tree that are hypothesized to have diversified under significantly different rates. In our case, we explored two tree partitions: the largely heterostylous clade /Primula (ca. 82% of its extant species are heterostylous; >99% of all heterostylous primroses are part of this clade) and the almost exclusively non-heterostylous grade /Androsace + /Soldanella (ca. 99% of its taxa are non-heterostylous). BayesRate estimates the fit of the data (the branching times in the phylogeny) to a given diversification model/hypothesis (constant-rate birth-death models [39] for pre-specified partitions of the tree). Specifically, the marginal likelihood of each diversification model is first estimated using thermodynamic integration [62], and then the relative support for alternate diversification models is assessed using Bayes factors. We explored the fit of four diversification-rate models to the primrose tree: Model 1 constrained speciation and extinction rates between tree partitions to be equal; Model 2 constrained speciation rates to be equal between tree partitions but allowed extinction rates to differ; Model 3 constrained extinction rates to be equal between tree partitions but allowed speciation rates to differ; Model 4 allowed both speciation and extinction rates to differ between tree partitions. In our BayesRate analyses, we assumed exponential priors on

speciation and extinction rate parameters. We used MCMC to estimate the marginal likelihood for each diversification model: each chain used thermodynamic integration with six stepping stones spanning the prior and posterior. Each MCMC simulation was performed on a sample of 100 trees from the posterior distribution of trees estimated under the UCLN and UCEXP relaxed-clock modes, with 10,000 post-burnin cycles per tree, sampling every 10^{th} cycle. Inferences were corrected for unsampled taxa by setting the proportion of extant species sampled for the phylogeny to 0.340 and 0.412 for the heterostylous and non-heterostylous tree partitions, respectively (Table S4). Similar results were obtained when repeating the analyses after excluding all of the ca. 18% non-heterostylous species in /Primula. Our BayesRate analyses indicate significant support for a model that includes separate extinction rates for the heterostylous and non-heterostylous tree partitions (Table S3).

State-associated speciation and extinction rate analyses—Character-state associated speciation and extinction rates were estimated using BiSSE [40], implemented in the R package diversitree v. 0.9-6 [41], which allows for assessing the effects of heterostyly on diversification across the tree. Unlike the BayesRate analyses, BiSSE more fully accommodates uncertainty in character history by jointly estimating speciation, extinction and transition rates. On the other hand, BiSSE does not allow robust Bayesian model selection/hypothesis testing (as implemented in BayesRate). Accordingly, analyses using these approaches complement each other, and similar results under these methods may increase our confidence in the inferences. Moreover, a recent simulation study demonstrated that the BiSSE model has limited power to detect state-specific differences in diversification rates when rates are strongly asymmetric and/or when character states in species are strongly biased [42]. These consideration motivate analyses using multiple methods. BiSSE analyses were conducted on two datasets: (i) family-level including all species, and (ii) including only species of /Primula. This was done to compare results across long evolutionary timescales at the family level, including both gains and losses of heterostyly, and on shorter evolutionary timescales, including probably mostly recent losses of heterostyly.

We performed analyses using BiSSE under four nested diversification models: Model 1 constrains speciation and extinction rates to be equal in both states (heterostyly/non-heterostyly); Model 2 constrains speciation rates to be equal in both states but allows extinction rates to vary; Model 3 constrains extinction rates to be equal in both states but allows speciation rates to vary; Model 4 allows both speciation and extinction to vary in both states. For each of the four diversification models, we performed two analyses: in the first, we assumed equal transition rates among states (i.e., the rate of gain and loss of heterostyly was constrained to be equal: $q_{01} = q_{10}$); in the second, we allowed transition rates among states to vary (estimating q_{01} and q_{10} separately). We performed

maximum-likelihood estimates under each of these 8 models on each of 100 trees sampled from the posterior distribution. In all analyses, we assumed character-coding scheme 2. We assessed the relative fit of the 8 models to the data by calculating differences in AIC scores, which penalizes likelihood for the number of free model parameters, and AIC weights, which allows for approximating a confidence set of models (*i.e.*, the set of models that jointly (approximately) represent those supported by the data).

We also performed Bayesian analyses under the unconstrained BiSSE model (Model 4) at the family level, averaging inferences over a sample of 100 trees, running the MCMC simulation for 220 iterations of slice sampling per tree (discarding the first 20 samples per tree as burn in). The effective sample size for most parameters was greater than of 200, or otherwise >100. We specified relatively diffuse priors for the diversification-rate parameters—exponential densities with a mean equal to 2 times the log of the number of taxa divided by the root age (ca. 0.29) as suggested by [43]—although analyses using other priors did not qualitatively affect the results (not shown). We adjusted the window size for slice sampling following recommendations in the diversitree manual. We plotted distributions of difference between non-heterostyly and heterostyly-associated rates under the unconstrained model, and determined if the 95% interval of highest posterior density included 0 (as suggested by [43]), to assess congruence between the Bayesian and the ML analyses. Results of all BiSSE analyses are provided in Fig. 3 (main text), Fig. S2, and Table S3.

Testing for confounding effects of polyploidy—We performed additional analyses to explore the possibility that the increased diversification rates associated with the loss of heterostyly within /Primula might be due to confounding effects of polyploidy. The incidence of polyploidy is higher in species that have lost heterostyly [4,44], although there is no strict relationship between the two [45]. Since polyploidy may affect diversification rates [46], we wanted to make sure that the effects of heterostyly on diversification rates also hold when all polyploid species were excluded. Cytological data was assembled from counts published in the International Plant Chromosome Number Index, (http://www.tropicos.org/Project/IPCN), taxonomic sources listed in note 1 of Table S4, and [47,48]. Data was unavailable for 71 of 265 taxa. Analytical pipelines have been developed that use probabilistic models of chromosome number evolution [49] to explicitly locate events of polyploidization on a tree based on haploid chromosome numbers (ChromEvol; http://www.tau.ac.il/~itaymay/cp/chromEvol/). However, these methods were computationally too demanding due to the size of our dataset. Moreover, as explained in the ChromEvol manual, it may produce unreliable results when many species have missing data. In stead, all species with sporophytic chromosome numbers larger than $2n = 24$ were scored as polyploid. The rationale for this cut-off

is that diploid numbers are known to range from $2n = 16$ to $2n = 24$ [1,4]; http://www.tropicos.org/Project/IPCN. This procedure also removed (paleo-)polyploids with suspected strongly diploidized inheritance (e.g. in *Primula* sect. *Auricula*; [4]).

Of the 80 species thus excluded based on their chromosome number (37 from /Primula, 38 from /Androsace, 5 from /Soldanella), 22 were scored as heterostylous; of the 58 excluded non-heterostylous species, 16 were part of the /Primula clade. These numbers illustrate that polyploidy is a general evolutionary phenomenon in Primulaceae that is not restricted to, but nevertheless more common in non-heterostylous species. The same set of BiSSE analyses (1,600 total) as for the full datasets were performed, i.e., maximum-likelihood analyses for 100 trees from each of UCLN and UCEXP dating analyses, for /Primula and for the family-level data, for the four diversification models. Analyses had unconstrained transition-rate parameters (constraining them was not supported by AIC scores; not shown), and had sampling fractions set to account for the excluded species. Results of BiSSE analyses at the family level excluding polyploids are congruent with those on the full dataset: heterostyly is associated with increased diversification due to lower extinction (Table S3D). Similarly, within /Primula, the support for differential extinction rates is greatly diminished (Table S3E), as in the full dataset. In contrast to results based on the dataset that included polyploids, however, inferences under fully constrained models (where heterostyly has no effect on diversification rates) are now strongly rejected only under the UCLN dating analysis; results under the UCEXP analysis indicate similar support for the model with state-specific speciation rates and state-independent diversification rates (Table S3E). This latter result is probably due to the loss of power associated with the reduced number of number of species [42]. Comparing results where polyploids are excluded to those where polyploids were included indicates that polyploidy does not confound the effect of heterostyly on the inferred patterns of diversification in Primulaceae, although it may contribute to driving higher rates of diversification over shorter time scales after the loss of heterostyly within /Primula.

To further test for possible confounding effects of polyploidy, we also performed a MultiState Speciation and Extinction (MuSSE) analysis, an expansion of BiSSE allowing for more than two states, implemented in diversitree [50]. In principle, MuSSE allows the effects of polyploidy and heterostyly to be assessed without excluding data. In practice, however, it may be difficult to reliably perform inference under this very parameter-rich MuSSE model. Each species was assigned to one of four states, based on the chromosome count data available as explained above: (1) diploid and non-heterostylous; (2) diploid and heterostylous; (3) polyploid and non-heterostylous, and; (4) polyploid and heterostylous. Species with missing data were scored as "NA". We note that the assignment of di- vs. polyploidy to species is associated with considerable uncertainty, because

chromosome numbers for many species are unknown, or could not be verified from original sources. In addition, effects of missing data of states on the results of MuSSE analyses are poorly understood. Thus, we stress that in these analyses, the effects of "polyploidy" on diversification rates should be interpreted cautiously.

Full MuSSE models contain 4 speciation rates, 4 extinction rates, and 12 possible transition rates, but were impossible to fit reliably, as solve algorithms used by MuSSE in diversitree indicated maximum likelihood searches in fact reached saddle points. Accordingly, it was necessary to reduce model complexity. We therefore constrained the **Q**-matrix to only allow gains and losses of heterostyly (4 parameters: $q_{12,}$ $q_{21,}$ $q_{34,}$ q_{43}) and gains and losses of polyploidy (4 parameters: q_{13}, q_{31}, q_{24}, q_{42}). Simultaneous changes of polyploidy and heterostyly were not permitted; *i.e.*, q_{14}, q_{41}, q_{23}, q_{32} were set to zero. Preliminary model-selection analyses indicated that constraining the polyploidy-loss rate (q_{31}, q_{42}) or gain rate (q_{13}, q_{24}, respectively) to zero was not supported by **Δ**AIC scores. However, a comprehensive analysis to determine the optimal model was not possible because the most complex models did not reliably converge. We used subplex optimization with 100,000 iterations rather than the default of 10,000 to increase confidence in the accuracy of the parameter estimation at the expense of making each ML search computationally highly demanding. For both 100 trees of the posterior distributions of the UCLN and UCEXP relaxed-clock model analyses, we fitted the constrained MuSSE model and determined mean ± interquartile range of all parameters for the 265-taxon Primulaceae dataset. It was not possible to reliably fit MuSSE models on the smaller dataset (/Primula alone could not be analyzed), probably because the information contained in the data was insufficient to reliably estimate values for the large number of parameters in MuSSE models.

We confirmed the hypothesis that speciation rates across ploidy levels were similar between heterostylous and non-heterostylous lineages (Table S3F): interquartile ranges of λ_{state_1} and λ_{state_2} overlap, as do those of λ_{state_3} and λ_{state_4}. Similarly, we confirmed that across ploidy levels, extinction rates of heterostylous lineages are lower ($\mu_{state\_1} > \mu_{state\_2}$; $\mu_{state\_3} > \mu_{state\_4}$) and that net diversification rates of heterostylous lineages are higher ($[\lambda_{state\_2} - \mu_{state\_2}] > [\lambda_{state\_1} - \mu_{state\_1}]$; $[\lambda_{state\_4} - \mu_{state\_4}] > [\lambda_{state\_3} - \mu_{state\_3}]$) than those of non-heterostylous lineages. Thus, heterostyly had a net positive effect on diversification rates among both diploids and polyploids. We note that when taken at face value, results of MuSSE analyses suggest that among non-heterostylous lineages especially polyploid (state 3) rather than diploid species (state 1) experience relatively high extinction rates. However, the incompleteness of data on ploidy levels and the difficulty of statistically evaluating the best way to reduce model complexity make us reluctant to put emphasis on these results. Despite this uncertainty, we can confirm that analyses accounting for polyploidy are congruent with those that do not.

Cross-validated posterior predictive diversity analyses—To complement the diversification-rate analyses described above, which assume that extinction rates can be reliably estimated, we used the approach of [51] in using Cross-Validated Predictive Diversity Densities (CVPDD). CVPDD exploits the marginal posterior probability of the timing of the evolution of heterostyly, *t*, and the marginal posterior probability for the diversification rate in the non-heterostylous tree partition, *r*, to generate the predictive probability distribution of species, $E(n \mid t, r)$, that we would expect to observe if the heterostylous subclade diversified under the background diversification rate. The realized species diversity is then compared to this predictive diversity distribution to assess whether rates of diversification in heterostylous species differs significantly from their non-heterostylous relatives. The fully Bayesian nature of the method has the advantage that it can adequately incorporate the phylogenetic uncertainty (in the timing of the event and the background diversification rate), while only estimating a very modest number of parameters from the data, providing a robust inference framework.

Since the timing of the origin of heterostyly, *t*, depends on the phylogenetic position for the evolution of heterostyly (the oldest node inferred to be heterostylous), we considered two scenarios: the first infers the origin of heterostyly in the crown node of /Primula (node c in Fig. 2; t_{crown}); and the alternative scenario in which heterostyly evolved at the stem node of /Primula (our model-based character history analyses suggest both scenarios are plausible: node b in Fig. 2; t_{stem}). The posterior estimates for t_{stem} and t_{crown} were obtained from two separate BEAST analyses that were identical to the BEAST analyses described above, with the exception that the normal distribution at the root was substituted for the point estimate of highest posterior probability of the *Androsace-Primula* split in the Ericales analyses (limiting phylogenetic uncertainty to that stemming from the sequence data rather than that due to limited fossil availability), and all proposals that operate on the treeModel.rootHeight parameter were disabled. The background diversification rate, *r*, was extracted from separate BEAST analyses that excluded the /Primula clade, with settings as described for the Primulaceae dataset, except that we used a Yule prior for the branching process (i.e. pure birth), ran the six runs for 13,333,000 generations, and excluded 25% as burnin to obtain 10,000 samples. Again, we ran two parallel sets of analyses using UCLN and UCEXP relaxed clocks.

The Predictive Diversity Density was calculated using Equation 3 of [51] and Monte Carlo integration executed in R, by combining each posterior distribution of *r* (based on UCLN and UCEXP clocks) with the corresponding posterior distributions of t_{crown} and t_{stem}. Posterior predictive p-values were obtained by determining the fraction of the distribution *E* that was larger than the observed number of heterostylous species in /Primula (i.e.

≥ 457, see Table S4). Results of the CVPDD analyses are presented in Fig. S3 and indicate that the realized species diversity of the heterostylous clade /Primula is significantly larger than expected from the background diversification rate.

Species distributions in the Eastern Himalayan region—In theory, it could be possible that the higher rate of species diversification in /Primula can be explained by ecological opportunities in the Eastern Himalayan region alone, as opposed to the occurrence of heterostyly, if /Primula would be disproportionally exposed to those ecological opportunities, or if heterostyly would be underrepresented among the species in the Eastern Himalayan region. To show that this possibility is not supported by data, we tally numbers from Flora of China [5] (comprehensive for Primulaceae for a large part of the Sino-Himalayan region, and a good proxy for the whole region) for the three clades: largely heterostylous /Primula and largely non-heterostylous /Androsace and /Soldanella. We calculate expected numbers using the 99% confidence interval of binomial probability densities.

- Is the proportion of species in the Sino-Himalayan region different among clades?

Among the 556 species in /Primula (Table S4), 301 (54.1 %) are in Flora of China. Based on a probability of 54.1% to occur in China, we expect that of the 183 species in /Androsace + /Soldanella, between 82 and 116 occur in China. Indeed, there are 84 species in /Androsace and /Soldanella in Flora of China. Hence, in the Eastern Himalayan region, species are similarly represented from within and from outside the largely heterostylous clade /Primula.

- Is the proportion of non-heterostylous species different in the Sino-Himalayan region?

Among the 738 species total in Primulaceae (Table S4), 279 (37.8 %) are non-heterostylous, and among the 556 species in /Primula, 101 are non-heterostylous (17.8 %). How many of the 385 species in China in total and how many of the 301 species in /Primula in China do we expect to be non-heterostylous? Based on a global probability of 37.8% and a /Primula-specific probability of 17.8 % of non-heterostyly, we expect between 121 and 170 species total and 37 to 71 species in /Primula to be non-heterostylous and to occur in China. That is slightly more than the observed 101 species total and 28 species in /Primula that are non-heterostylous in China. Hence, the proportion of heterostylous and non-heterostylous species in the Sino-Himalayan region is slightly skewed against the hypothesis that heterostyly is underrepresented within the Eastern Himalayan region.

In summary, the heterostylous and non-heterostylous clades have similar fractions of species inside and outside the Sino-Himalayan region, and the proportion of species lacking heterostyly in /Primula in the Sino-Himalaya is slightly lower, rather than higher, than expected. This is congruent with the notion of heterostylous species benefitting relatively more from the extrinsic opportunities the environment offers for diversification,

reinforcing the importance of heterostyly in explaining differential diversification rates across Primulaceae, as explained in the discussion.

References

1. Schneeweiss, G. M., Schönswetter, P., Kelso, S. & Niklfeld, H. 2004 Complex biogeographic patterns in *Androsace* (Primulaceae) and related genera: evidence from phylogenetic analyses of nuclear internal transcribed spacer and plastid trnL-F sequences. *Syst. Biol.* **53**, 856–876. (doi:10.1080/10635150490522566)

2. Mast, A. R., Kelso, S. & Conti, E. 2006 Are any primroses (*Primula*) primitively monomorphic? *New Phytol.* **171**, 605–616. (doi:10.1111/j.1469-8137.2006.01700.x)

3. Yan, H. F., He, C. H., Peng, C. I., Hu, C.-M. & Hao, G. 2010 Circumscription of *Primula* subgenus *Auganthus* (Primulaceae) based on chloroplast DNA sequences. *J. Syst. Evol.* **48**, 123–132.

4. Richards, A. J. 2003 *Primula*. 2nd edn. Portland, Oregon: Timber Press.

5. Hu, C.-M. & Kelso, S. 1996 Primulaceae. In *Flora of China 15: Myrsinaceae through Loganiaceae* (eds Z. Y. Wu & P. H. Ravens), pp. 39–189. Science Press, Beijing, and Missouri Botanical Garden Press, St. Louis.

6. Ernst, A. 1962 Stammesgeschichtliche Untersuchungen zum Heterostylie-Problem - 7. Stand des Nachweises monomorpher Arten, homostyler Sippen und anderer genetisch bedingter Abweichungen vom 'klassischen' Blütendimorphismus in den Sektionen der Gattung *Primula*. *Arch. Julius Klaus Stift. Vererbungsforsch. Sozialanthropol. Rassenhyg. Zür.* **37**, 1–127.

7. Mast, A. R., Feller, D. M. S., Kelso, S. & Conti, E. 2004 Buzz-pollinated *Dodecatheon* originated from within the heterostylous *Primula* subgenus *Auriculastrum* (Primulaceae): a seven-region cpDNA phylogeny and its implications for floral evolution. *Am. J. Bot.* **91**, 926–942. (doi:10.3732/ajb.91.6.926)

8. Taberlet, P., Gielly, L., Pautou, G. & Bouvet, J. 1991 Universal primers for amplification of three non-coding regions of chloroplast DNA. *Plant Mol. Biol.* **17**, 1105–1109.

9. Sang, T., Crawford, D. & Stuessy, T. 1997 Chloroplast DNA phylogeny, reticulate evolution, and biogeography of *Paeonia* (Paeoniaceae). *Am. J. Bot.* **84**, 1120.

10. Jordan, W. C., Courtney, M. W. & Neigel, J. E. 1996 Low levels of intraspecific genetic variation at a rapidly evolving chloroplast DNA locus in North American duckweeds (Lemnaceae). *Am. J. Bot.*, 430–439.

11. Baum, D. A., Alverson, W. S. & Nyffeler, R. 1998 A durian by any other name: taxonomy and nomenclature of the core Malvales. *Harvard Pap. Bot.* **3**, 315–330.

12. Edgar, R. C. 2004 MUSCLE: multiple sequence alignment with high accuracy and high throughput. *Nucleic Acids Res.* **32**, 1792–1797. (doi:10.1093/nar/gkh340)

13. Drummond, A. J. & Rambaut, A. 2007 BEAST: Bayesian evolutionary analysis by sampling trees. *BMC Evol Biol* **7**, 214. (doi:10.1186/1471-2148-7-214)

14. Posada, D. & Buckley, T. R. 2004 Model selection and model averaging in phylogenetics: advantages of Akaike information criterion and Bayesian approaches over likelihood ratio tests. *Syst. Biol.* **53**, 793–808.

(doi:10.1080/10635150490522304)

15. Ronquist, F. & Huelsenbeck, J. P. 2003 MrBayes 3: Bayesian phylogenetic inference under mixed models. *Bioinformatics* **19**, 1572–1574. (doi:10.1093/bioinformatics/btg180)

16. Posada, D. & Crandall, K. A. 1998 MODELTEST: testing the model of DNA substitution. *Bioinformatics* **14**, 817–818.

17. Lemmon, A. R. & Moriarty, E. C. 2004 The importance of proper model assumption in Bayesian phylogenetics. *Syst. Biol.* **53**, 265–277. (doi:10.1080/10635150490423520)

18. Wilgenbusch, J. C., Warren, D. L. & Swofford, D. L. 2004 AWTY: A system for graphical exploration of MCMC convergence in Bayesian phylogenetic inference.

19. Yesson, C., Toomey, N. H. & Culham, A. 2009 Cyclamen: time, sea and speciation biogeography using a temporally calibrated phylogeny. *J. Biogeogr.* **36**, 1234–1252. (doi:10.1111/j.1365-2699.2008.01971.x)

20. Boucher, F. C., Thuiller, W., Roquet, C., Douzet, R., Aubert, S., Alvarez, N. & Lavergne, S. 2012 Reconstructing the origins of high-alpine niches and cushion life form in the genus *Androsace* s.l. (Primulaceae). *Evolution* **66**, 1255–1268. (doi:10.1111/j.1558-5646.2011.01483.x)

21. Dorofeev, P. I. 1963 Primulaceae. In *Oznovij Paleontologii* (ed A. L. Takhtajan), pp. 517–518. Moscow, Russia: Akademia Nauk.

22. Łańcucka-Środoniowa, M. 1966 Tortonian Flora from the 'Gdów Bay' in the South of Poland. *Acta Palaeobot* **7**, 3–135.

23. Łańcucka-Środoniowa, M. 1979 Macroscopic plant remains from the freshwater Miocene of the Nowy Sacz Basin (West Carpathians, Poland). *Acta Palaeobot* **20**, 3–117.

24. Czaja, A. 2003 Paläokarpologische Untersuchungen von Taphozönosen des Unter- und Mittelmiozäns aus dem Braunkohlentagebau Berzdorf/Oberlausitz (Sachsen). *Palaeontographica Abteilung B* **265**, 1–148.

25. Ho, S. Y. 2007 Calibrating molecular estimates of substitution rates and divergence times in birds. *J. Avian Biol.* **38**, 409–414. (doi:10.1111/j.2007.0908-8857.04168.x)

26. Knobloch, E. & Mai, D. H. 1986 Monographie der Früchte und Samen in der Kreide von Mitteleuropa. *Rozpravy ústredního ústavu geologickenho, Praha* **47**, 1–219.

27. Bremer, K. 2004 Molecular phylogenetic dating of asterid flowering plants shows early Cretaceous diversification. *Syst. Biol.* **53**, 496–505. (doi:10.1080/10635150490445913)

28. Magallon, S. & Sanderson, M. J. 2001 Absolute diversification rates in angiosperm clades. *Evolution* **55**, 1762–1780.

29. Doyle, J. A. & Hotton, C. L. 1991 Diversification of early angiosperm pollen in a cladistic context. In *Pollen and Spores: Pattern of Diversification* (eds S. Blackmore & S. H. Barnes), pp. 165–195. Oxford: Clarendon Press.

30. Schaeppi, H. 1934 Untersuchungen über die Narben- und Antheren-Stellung in den Blüten der Primulaceen. *Arch. Julius Klaus Stift. Vererbungsforsch. Sozialanthropol. Rassenhyg. Zür.* **10**, 133–236.

31. Schaeppi, H. 1935 Zur Kenntnis der Heterostylie von Gregoria vitaliana Duby. *Ber. Schweiz. Bot. Ges.* **44**, 109–132.

32. Huang, Y., Zhang, C. Q., Blackmore, S., Li, D. Z. & Wu, Z. K. 2006 A preliminary study on pollination biology of *Omphalogramma souliei* Franch. (Primulaceae), a species endemic to China. *Plant Syst. Evol.* **261**, 89–98. (doi:10.1007/s00606-006-0430-0)

33. Vos, J. M., Keller, B., Isham, S. T., Kelso, S. & Conti, E. 2012 Reproductive implications of herkogamy in homostylous primroses: variation during anthesis and reproductive assurance in alpine environments. *Funct. Ecol.* **26**, 854–865. (doi:10.1111/j.1365-2435.2012.02016.x)

34. Pagel, M. & Meade, A. 2006 BayesTraits.

35. Maddison, W. P. & Maddison, D. R. 2011 Mesquite.

36. Alfaro, M. E., Santini, F., Brock, C., Alamillo, H., Dornburg, A., Rabosky, D. L., Carnevale, G. & Harmon, L. J. 2009 Nine exceptional radiations plus high turnover explain species diversity in jawed vertebrates. *Proc. Natl. Acad. Sci. U.S.A.* **106**, 13410–13414. (doi:10.1073/pnas.0811087106)

37. Chan, K. M. A. & Moore, B. R. 2005 SYMMETREE: whole-tree analysis of differential diversification rates. *Bioinformatics* **21**, 1709–1710. (doi:10.1093/bioinformatics/bti175)

38. Silvestro, D., Schnitzler, J. & Zizka, G. 2011 A Bayesian framework to estimate diversification rates and their variation through time and space. *BMC Evol Biol* **11**, 311. (doi:10.1186/1471-2148-11-311)

39. Nee, S., May, R. M. & Harvey, P. H. 1994 The reconstructed evolutionary process. *Phil. Trans. R. Soc. B* **344**, 305–311.

40. Maddison, W. P., Midford, P. E. & Otto, S. P. 2007 Estimating a binary character's effect on speciation and extinction. *Syst. Biol.* **56**, 701–710. (doi:10.1080/10635150701607033)

41. FitzJohn, R. G. 2012 diversitree: comparative phylogenetic analyses of diversification.

42. Davis, M. P., Midford, P. E. & Maddison, W. 2013 Exploring power and parameter estimation of the BiSSE method for analyzing species diversification. *BMC Evol Biol* **13**, 38.

43. Johnson, M. T. J., FitzJohn, R. G., Smith, S. D., Rausher, M. D. & Otto, S. P. 2011 Loss of sexual recombination and segregation is associated with increased diversification in evening primroses. *Evolution* **65**, 3230–3240. (doi:10.1111/j.1558-5646.2011.01378.x)

44. Guggisberg, A., Mansion, G., Kelso, S. & Conti, E. 2006 Evolution of biogeographic patterns, ploidy levels, and breeding systems in a diploid-polyploid species complex of Primula. *New Phytol.* **171**, 617–632. (doi:10.1111/j.1469-8137.2006.01722.x)

45. Naiki, A. 2012 Heterostyly and the possibility of its breakdown by polyploidization. *Plant Spec. Biol.* **27**, 3–29. (doi:10.1111/j.1442-1984.2011.00363.x)

46. Mayrose, I., Zhan, S. H., Rothfels, C. J., Magnuson-Ford, K., Barker, M. S., Rieseberg, L. H. & Otto, S. P. 2011 Recently formed polyploid plants diversify at lower rates. *Science* **333**, 1257–1257. (doi:10.5061/dryad.6hf21))

47. Kress, A. 1984 Chromosomenzählung an verschiedenen Primulaceen. Teil A: *Androsace*. *Primulaceen-Studien* **3**, 1–32.

48. Fedorov, A. A. 1969 *Chromosome Numbers of Flowering Plants*. Komarov Botanical Institute, St. Petersburg.

49. Mayrose, I., Barker, M. S. & Otto, S. P. 2010 Probabilistic models of chromosome number evolution and the inference of polyploidy. *Syst. Biol.* **59**, 132–144. (doi:10.1093/sysbio/syp083)

50. FitzJohn, R. G. 2012 Diversitree: comparative phylogenetic analyses of diversification in R. *Methods in Ecology and Evolution* **3**, 1084–1092. (doi:10.1111/j.2041-210X.2012.00234.x)

51. Moore, B. R. & Donoghue, M. J. 2009 A Bayesian approach for evaluating the impact of historical events on rates of diversification. *Proc. Natl. Acad. Sci. U.S.A.* **106**, 4307–4312. (doi:10.1073/pnas.0807230106)

52. Kass, R. E. & Raftery, A. E. 1995 Bayes factors. *J. Am. Statist. Assoc.* **90**, 773–795.

53. Smith, G. & Lowe, D. 1997 *The Genus Androsace*. Pershore: The Alpine Garden Society.

54. Lidén, M. 2007 The genus *Dionysia* (Primulaceae), a synopsis and five new species. *Willdenowia* **37**, 37–61. (doi:10.3372/wi.37.37102)

55. Mast, A. & Reveal, J. 2007 Transfer of *Dodecatheon* to *Primula* (Primulaceae). *Brittonia* **59**, 79–82.

56. Zhang, L. B. & Kadereit, J. W. 2002 The systematics of *Soldanella* (Primulaceae) based on morphological and molecular (ITS, AFLPs) evidence. *Nord. J. Bot.* **22**, 129–169.

57. Ernst, A. 1938 Stammesgeschichtliche Untersuchungen zum Heterostylie-Problem. *Ber. Schweiz. Bot. Ges.* **48**, 85–238.

58. Ernst, A. 1959 Stammesgeschichtliche Untersuchungen zum Heterostylie-Problem. 5. *Arch. Julius Klaus Stift. Vererbungsforsch. Sozialanthropol. Rassenhyg. Zür.* **34**, 57–191.

59. Bentvelzen, P. A. J. 1962 Primulaceae. *Flora Maleisiana* **6**, 173–192.

60. Nylander, J.A., Ronquist, F., Huelsenbeck, J.P. & Nieves-Aldrey, J. 2004 Bayesian phylogenetic analysis of combined data. *Syst. Biol.* **53**, 47–67.

61. Koenen, E.J.M., et al. 2013 Exploring the tempo of species diversification in legumes. *South African J. Bot.* **89**, 19–30.

62. Lartillot, N. & Philippe, H. 2006 Computing Bayes factors using thermodynamic integration. *Syst. Biol.* **55**, 195–207.

Figure S1A

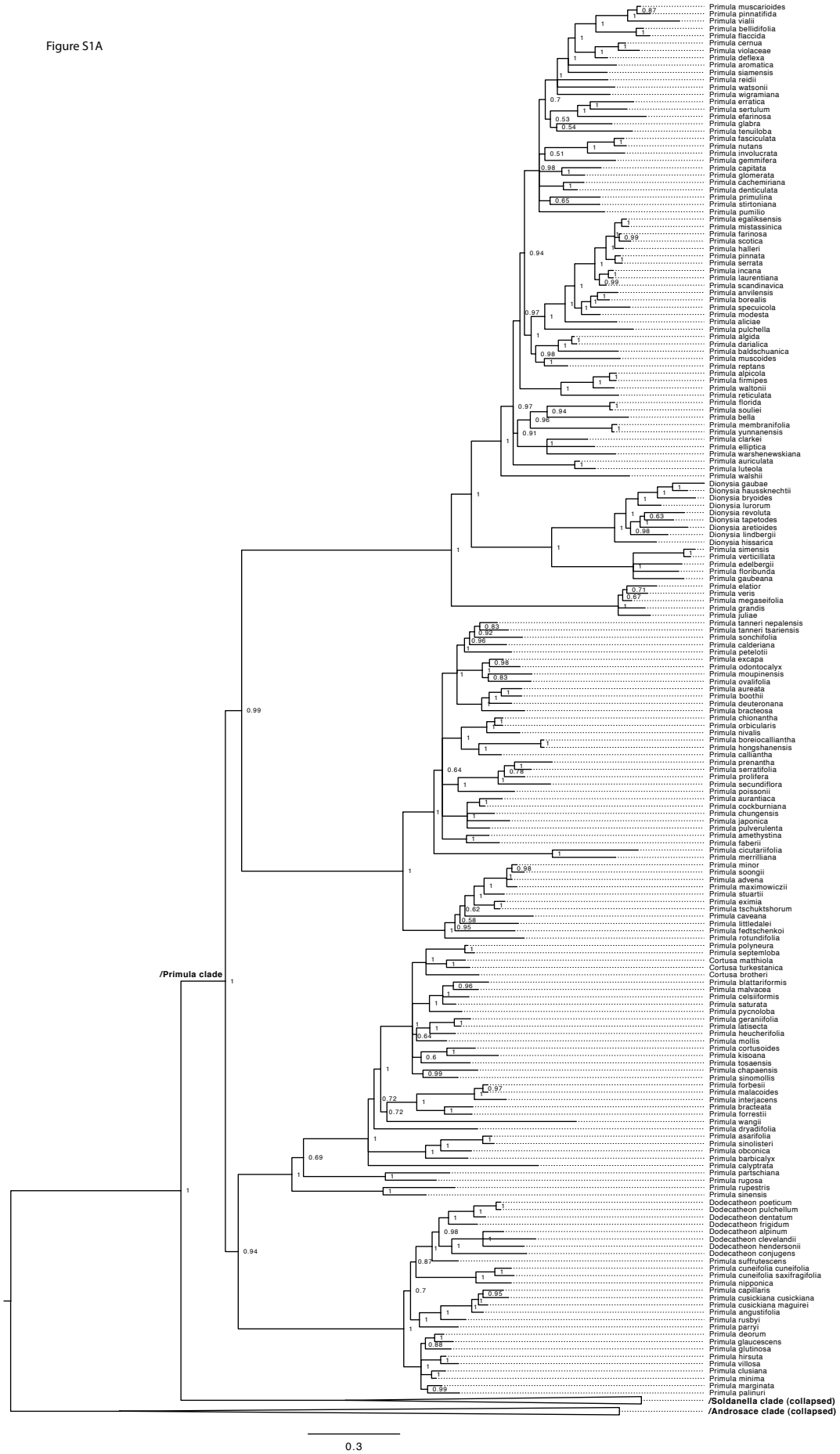
Primula muscarioides
Primula pinnatifida
Primula vialii
Primula bellidifolia
Primula flaccida
Primula cernua
Primula violaceae
Primula deflexa
Primula aromatica
Primula siamensis
Primula reidii
Primula watsonii
Primula wigramiana
Primula erratica
Primula sertulum
Primula efarinosa
Primula glabra
Primula tenuiloba
Primula fasciculata
Primula nutans
Primula involucrata
Primula gemmifera
Primula capitata
Primula glomerata
Primula cachemiriana
Primula denticulata
Primula primulina
Primula stirtoniana
Primula pumilio
Primula egaliksensis
Primula mistassinica
Primula farinosa
Primula scotica
Primula halleri
Primula pinnata
Primula serrata
Primula incana
Primula laurentiana
Primula scandinavica
Primula anvilensis
Primula borealis
Primula specuicola
Primula modesta
Primula aliciae
Primula pulchella
Primula algida
Primula darialica
Primula baldschuanica
Primula muscoides
Primula reptans
Primula alpicola
Primula firmipes
Primula waltonii
Primula reticulata
Primula florida
Primula souliei
Primula bella
Primula membranifolia
Primula yunnanensis
Primula clarkei
Primula elliptica
Primula warshenewskiana
Primula auriculata
Primula luteola
Primula walshii
Dionysia gaubae
Dionysia haussknechtii
Dionysia bryoides
Dionysia lurorum
Dionysia revoluta
Dionysia tapetodes
Dionysia aretioides
Dionysia lindbergii
Dionysia hissarica
Primula simensis
Primula verticillata
Primula edelbergii
Primula floribunda
Primula gaubeana
Primula elatior
Primula veris
Primula megaseifolia
Primula grandis
Primula juliae
Primula tanneri nepalensis
Primula tanneri tsariensis
Primula sonchifolia
Primula calderiana
Primula petelotii
Primula excapa
Primula odontocalyx
Primula moupinensis
Primula ovalifolia
Primula aureata
Primula boothii
Primula deuteronana
Primula bracteosa
Primula chionantha
Primula orbicularis
Primula nivalis
Primula boreiocalliantha
Primula hongshanensis
Primula calliantha
Primula prenantha
Primula serratifolia
Primula prolifera
Primula secundiflora
Primula poissonii
Primula aurantiaca
Primula cockburniana
Primula chungensis
Primula japonica
Primula pulverulenta
Primula amethystina
Primula faberii
Primula cicutariifolia
Primula merrilliana
Primula minor
Primula soongii
Primula advena
Primula maximowiczii
Primula stuartii
Primula eximia
Primula tschuktshorum
Primula caveana
Primula littledalei
Primula fedtschenkoi
Primula rotundifolia
Primula polyneura
Primula septemloba
Cortusa matthiola
Cortusa turkestanica
Cortusa brotheri
Primula blattariformis
Primula malvacea
Primula celsiiformis
Primula saturata
Primula pycnoloba
Primula geraniifolia
Primula latisecta
Primula heucherifolia
Primula mollis
Primula cortusoides
Primula kisoana
Primula tosaensis
Primula chapaensis
Primula sinomollis
Primula forbesii
Primula malacoides
Primula interjacens
Primula bracteata
Primula forrestii
Primula wangii
Primula dryadifolia
Primula asarifolia
Primula sinolisteri
Primula obconica
Primula barbicalyx
Primula calyptrata
Primula partschiana
Primula rugosa
Primula rupestris
Primula sinensis
Dodecatheon poeticum
Dodecatheon pulchellum
Dodecatheon dentatum
Dodecatheon frigidum
Dodecatheon alpinum
Dodecatheon clevelandii
Dodecatheon hendersonii
Dodecatheon conjugens
Primula suffrutescens
Primula cuneifolia cuneifolia
Primula cuneifolia saxifragifolia
Primula nipponica
Primula capillaris
Primula cusickiana cusickiana
Primula cusickiana maguirei
Primula angustifolia
Primula rusbyi
Primula parryi
Primula decorum
Primula glaucescens
Primula glutinosa
Primula hirsuta
Primula villosa
Primula clusiana
Primula minima
Primula marginata
Primula palinuri
/Soldanella clade (collapsed)
/Androsace clade (collapsed)
/Primula clade
0.3

Figure S1A (continued)

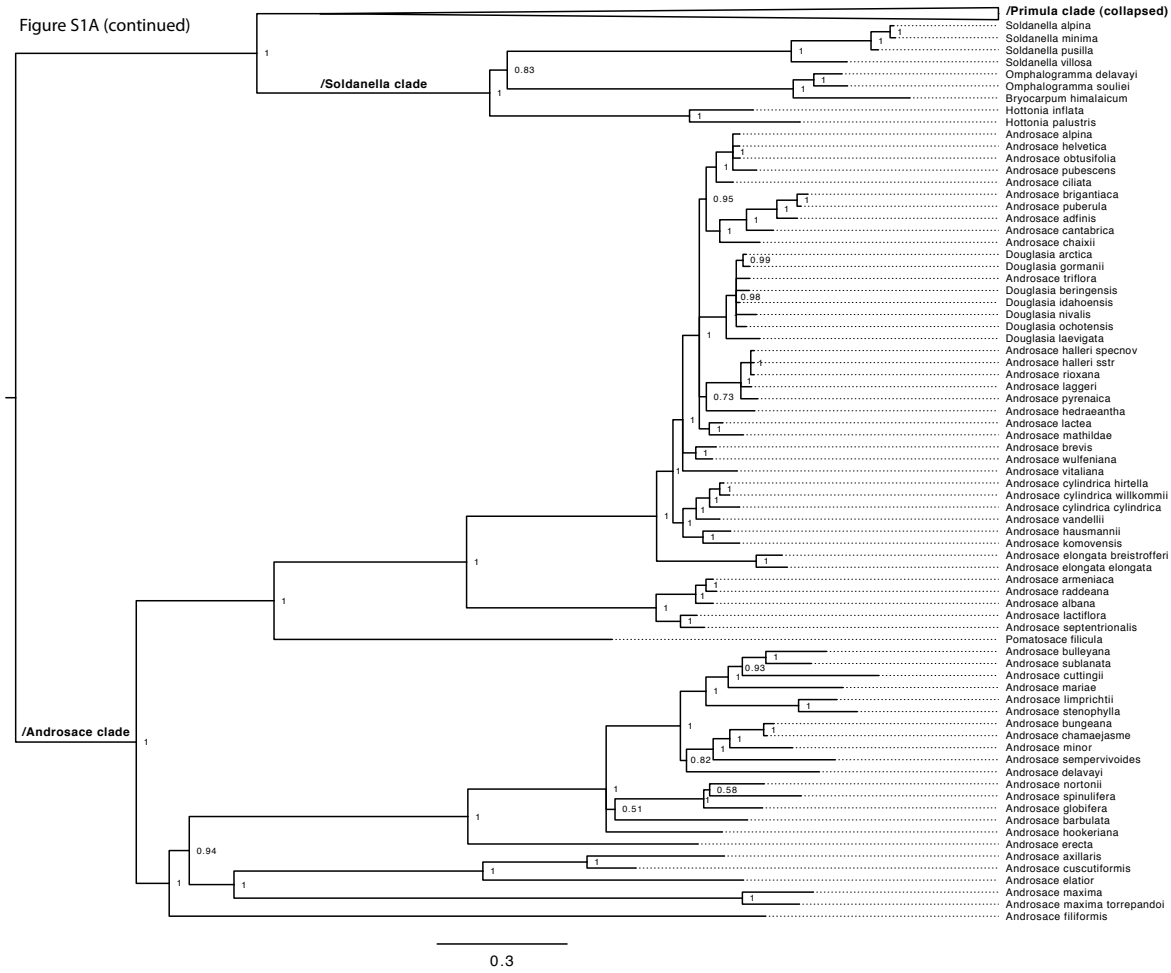

Figure S1B

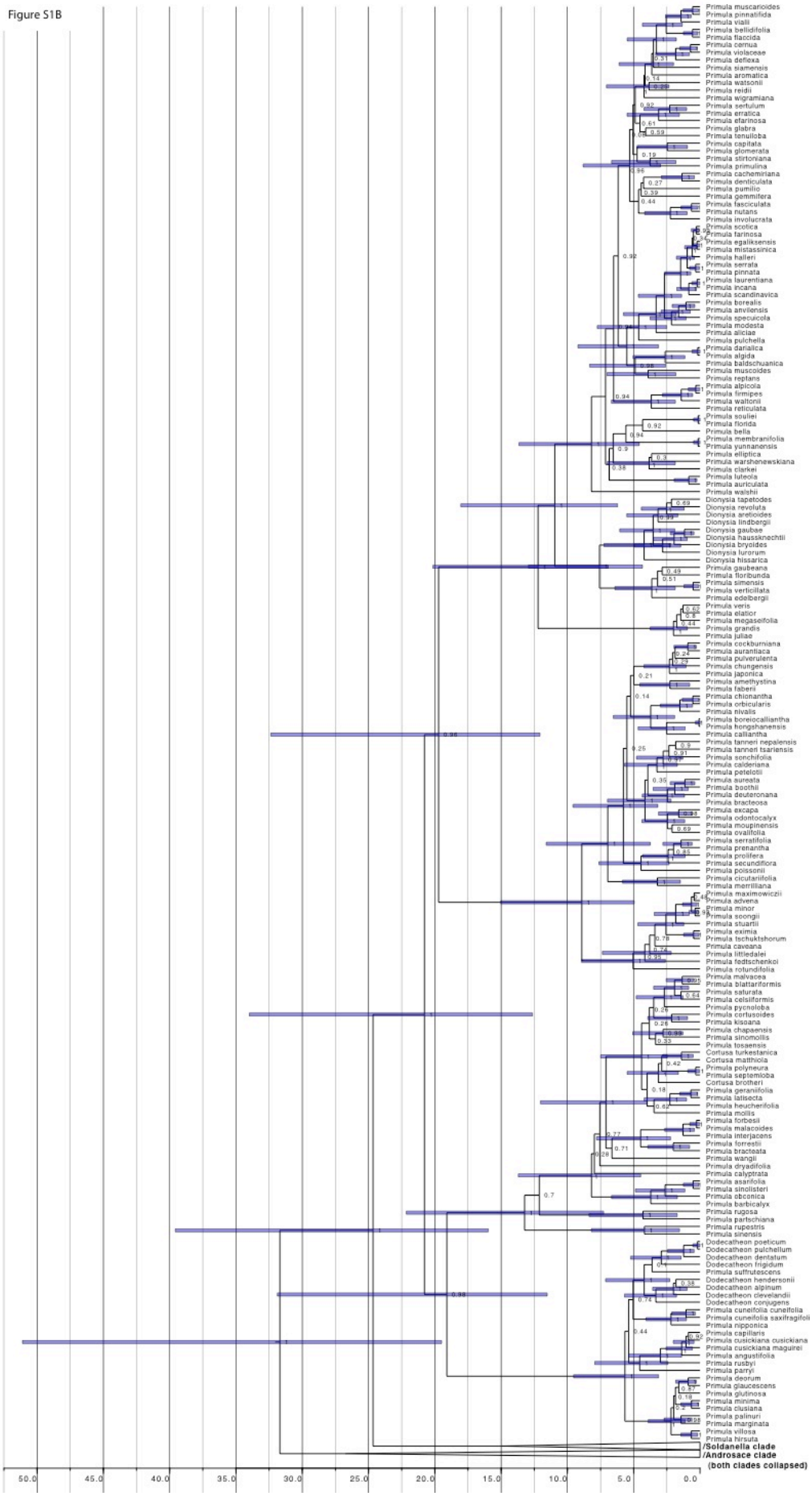
Primula muscarioides
Primula pinnatifida
Primula vialii
Primula bellidifolia
Primula flaccida
Primula cernua
Primula violacea
Primula deflexa
Primula siamensis
Primula aromatica
Primula watsonii
Primula reidii
Primula wigramiana
Primula sertulum
Primula erratica
Primula efarinosa
Primula glabra
Primula tenuiloba
Primula capitata
Primula glomerata
Primula stirtoniana
Primula primulina
Primula cachemiriana
Primula denticulata
Primula pumilio
Primula gemmifera
Primula fasciculata
Primula nutans
Primula involucrata
Primula scotica
Primula farinosa
Primula egaliksensis
Primula mistassinica
Primula halleri
Primula serrata
Primula pinnata
Primula laurentiana
Primula incana
Primula scandinavica
Primula borealis
Primula anvilensis
Primula specuicola
Primula modesta
Primula aliciae
Primula pulchella
Primula darialica
Primula algida
Primula baldschuanica
Primula muscoides
Primula reptans
Primula alpicola
Primula firmipes
Primula waltonii
Primula reticulata
Primula souliei
Primula florida
Primula bella
Primula membranifolia
Primula yunnanensis
Primula elliptica
Primula warshenewskiana
Primula clarkei
Primula luteola
Primula auriculata
Primula walshii
Dionysia tapetodes
Dionysia revoluta
Dionysia aretioides
Dionysia lindbergii
Dionysia gaubae
Dionysia haussknechtii
Dionysia bryoides
Dionysia lurorum
Dionysia hissarica
Primula gaubeana
Primula floribunda
Primula simensis
Primula verticillata
Primula edelbergii
Primula veris
Primula elatior
Primula megaseifolia
Primula grandis
Primula juliae
Primula cockburniana
Primula aurantiaca
Primula pulverulenta
Primula chungensis
Primula japonica
Primula amethystina
Primula faberii
Primula chionantha
Primula orbicularis
Primula nivalis
Primula boreiocalliantha
Primula hongshanensis
Primula calliantha
Primula tanneri nepalensis
Primula tanneri tsariensis
Primula sonchifolia
Primula calderiana
Primula petelotii
Primula aureata
Primula boothii
Primula deuteronana
Primula bracteosa
Primula excapa
Primula odontocalyx
Primula moupinensis
Primula ovalifolia
Primula serratifolia
Primula prenantha
Primula prolifera
Primula secundiflora
Primula poissonii
Primula cicutariifolia
Primula merrilliana
Primula maximowiczii
Primula advena
Primula minor
Primula soongii
Primula stuartii
Primula eximia
Primula tschuktshorum
Primula caveana
Primula littledalei
Primula fedtschenkoi
Primula rotundifolia
Primula malvacea
Primula blattariformis
Primula saturata
Primula celsiiformis
Primula pycnoloba
Primula cortusoides
Primula kisoana
Primula chapaensis
Primula sinomollis
Primula tosaensis
Cortusa turkestanica
Cortusa matthiola
Primula polyneura
Primula septemloba
Cortusa brotheri
Primula geraniifolia
Primula latisecta
Primula heucherifolia
Primula mollis
Primula forbesii
Primula malacoides
Primula interjacens
Primula forrestii
Primula bracteata
Primula wangii
Primula dryadifolia
Primula calyptrata
Primula asarifolia
Primula sinolisteri
Primula obconica
Primula barbicalyx
Primula rugosa
Primula partschiana
Primula rupestris
Primula sinensis
Dodecatheon poeticum
Dodecatheon pulchellum
Dodecatheon dentatum
Dodecatheon frigidum
Primula suffrutescens
Dodecatheon hendersonii
Dodecatheon alpinum
Dodecatheon clevelandii
Dodecatheon conjugens
Primula cuneifolia cuneifolia
Primula cuneifolia saxifragifoli
Primula nipponica
Primula capillaris
Primula cusickiana cusickiana
Primula cusickiana maguirei
Primula angustifolia
Primula rusbyi
Primula parryi
Primula deorum
Primula glaucescens
Primula glutinosa
Primula minima
Primula clusiana
Primula palinuri
Primula marginata
Primula villosa
Primula hirsuta
/Soldanella clade
/Androsace clade
(both clades collapsed)
50.0
45.0
40.0
35.0
30.0
25.0
20.0
15.0
10.0
5.0
0.0

Figure S1B (continued)

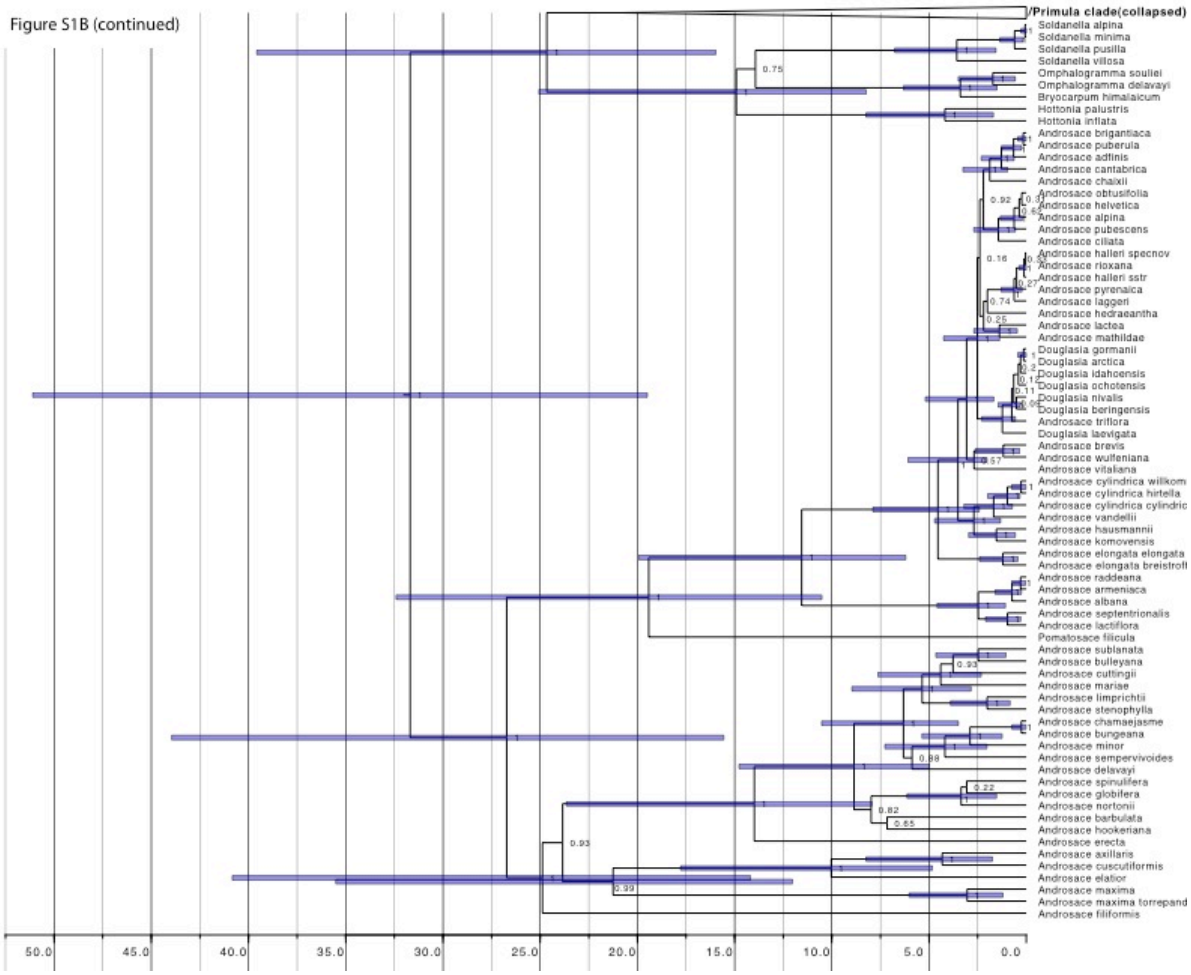

Figure S1C

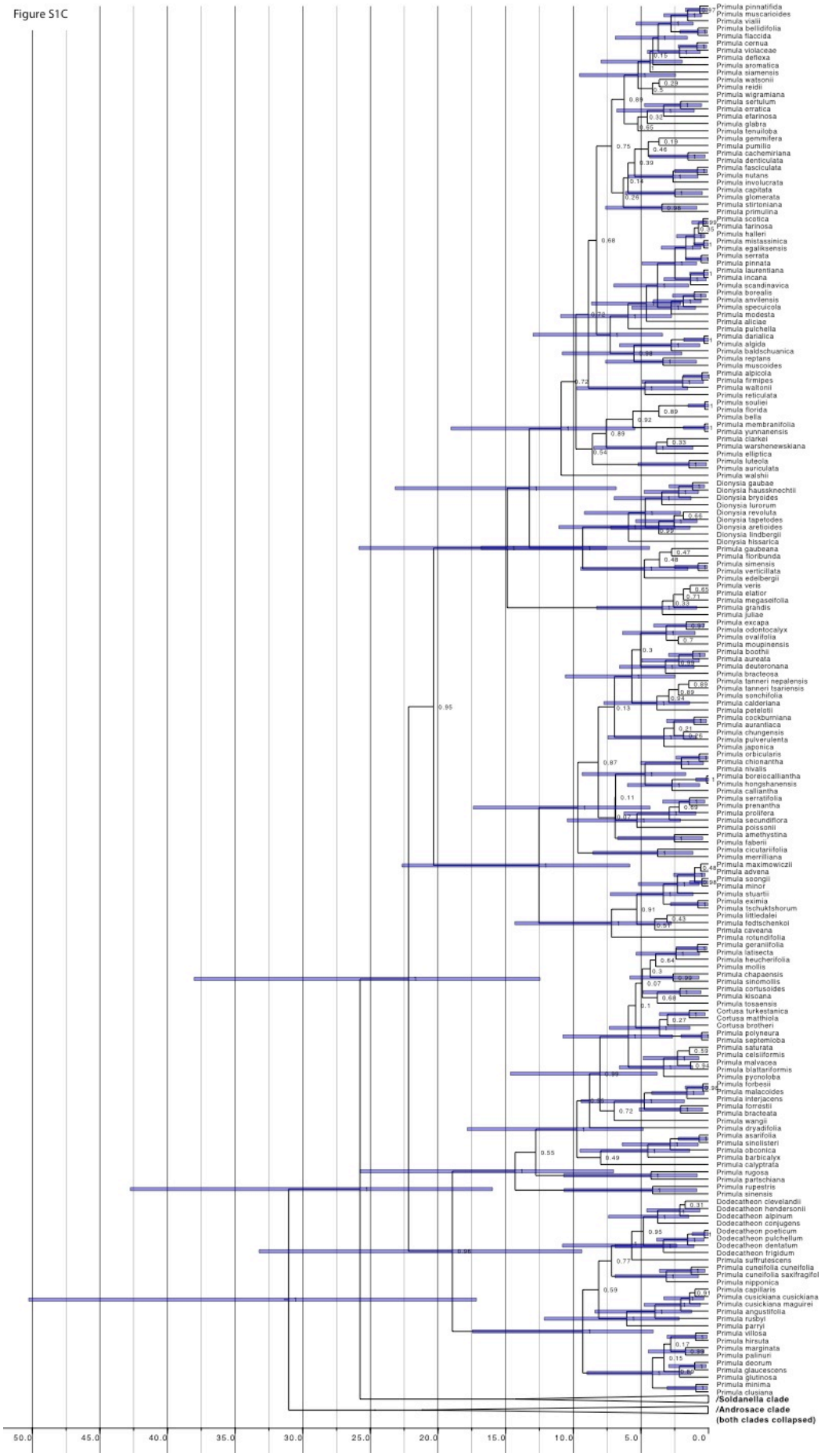
Primula pinnatifida
Primula muscarioides
Primula vialii
Primula bellidifolia
Primula flaccida
Primula cernua
Primula violaceae
Primula deflexa
Primula aromatica
Primula siamensis
Primula watsonii
Primula reidii
Primula wigramiana
Primula sertulum
Primula erratica
Primula efarinosa
Primula glabra
Primula tenuiloba
Primula gemmifera
Primula pumilio
Primula cachemiriana
Primula denticulata
Primula fasciculata
Primula nutans
Primula involucrata
Primula capitata
Primula glomerata
Primula stirtoniana
Primula primulina
Primula scotica
Primula farinosa
Primula halleri
Primula mistassinica
Primula egaliksensis
Primula serrata
Primula pinnata
Primula laurentiana
Primula incana
Primula scandinavica
Primula borealis
Primula anvilensis
Primula specuicola
Primula modesta
Primula aliciae
Primula pulchella
Primula darialica
Primula algida
Primula baldschuanica
Primula reptans
Primula muscoides
Primula alpicola
Primula firmipes
Primula waltonii
Primula reticulata
Primula souliei
Primula florida
Primula bella
Primula membranifolia
Primula yunnanensis
Primula clarkei
Primula warshenewskiana
Primula elliptica
Primula luteola
Primula auriculata
Primula walshii
Dionysia gaubae
Dionysia haussknechtii
Dionysia bryoides
Dionysia lurorum
Dionysia revoluta
Dionysia tapetodes
Dionysia aretioides
Dionysia lindbergii
Dionysia hissarica
Primula gaubeana
Primula floribunda
Primula simensis
Primula verticillata
Primula edelbergii
Primula veris
Primula elatior
Primula megaseifolia
Primula grandis
Primula juliae
Primula excapa
Primula odontocalyx
Primula ovalifolia
Primula moupinensis
Primula boothii
Primula aureata
Primula deuteronana
Primula bracteosa
Primula tanneri nepalensis
Primula tanneri tsariensis
Primula sonchifolia
Primula calderiana
Primula petelotii
Primula cockburniana
Primula aurantiaca
Primula chungensis
Primula pulverulenta
Primula japonica
Primula orbicularis
Primula chionantha
Primula nivalis
Primula borelocalliantha
Primula hongshanensis
Primula calliantha
Primula serratifolia
Primula prenantha
Primula prolifera
Primula secundiflora
Primula poissonii
Primula amethystina
Primula faberi
Primula cicutariifolia
Primula merrilliana
Primula maximowiczii
Primula advena
Primula soongii
Primula minor
Primula stuartii
Primula eximia
Primula tschuktshorum
Primula littledalei
Primula fedtschenkoi
Primula caveana
Primula rotundifolia
Primula geraniifolia
Primula latisecta
Primula heucherifolia
Primula mollis
Primula chapaensis
Primula sinomollis
Primula cortusoides
Primula kisoana
Primula tosaensis
Cortusa turkestanica
Cortusa matthiola
Cortusa brotheri
Primula polyneura
Primula septemloba
Primula saturata
Primula celsiiformis
Primula malvacea
Primula blattariformis
Primula pycnoloba
Primula forbesii
Primula malacoides
Primula interjacens
Primula forrestii
Primula bracteata
Primula wangii
Primula dryadifolia
Primula asarifolia
Primula sinolisteri
Primula obconica
Primula barbicalyx
Primula calyptrata
Primula rugosa
Primula partschiana
Primula rupestris
Primula sinensis
Dodecatheon clevelandii
Dodecatheon hendersonii
Dodecatheon alpinum
Dodecatheon conjugens
Dodecatheon poeticum
Dodecatheon pulchellum
Dodecatheon dentatum
Dodecatheon frigidum
Primula suffrutescens
Primula cuneifolia cuneifolia
Primula cuneifolia saxifragifol
Primula nipponica
Primula capillaris
Primula cusickiana cusickiana
Primula cusickiana maguirei
Primula angustifolia
Primula rusbyi
Primula parryi
Primula villosa
Primula hirsuta
Primula marginata
Primula palinuri
Primula deorum
Primula glaucescens
Primula glutinosa
Primula minima
Primula clusiana
/Soldanella clade
/Androsace clade
(both clades collapsed)
50.0
45.0
40.0
35.0
30.0
25.0
20.0
15.0
10.0
5.0
0.0

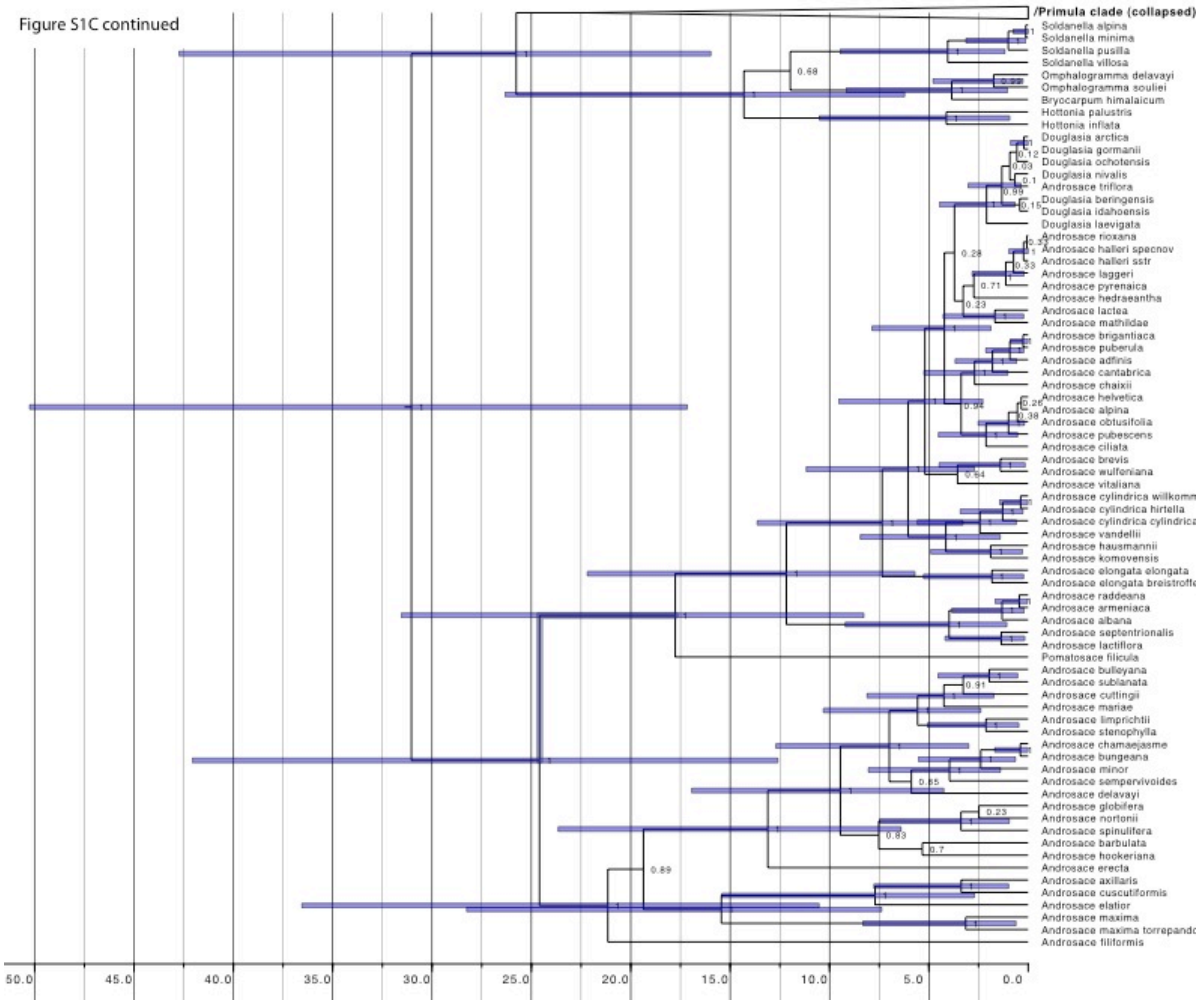

Fig. S1. Phylogenetic relationships within Primulaceae s.str. inferred with MrBayes (A) and BEAST using the uncorrelated relaxed lognormal (UCLN; B) and exponential (UCEXP; C) relaxed-clock models. (A) Majority rule consensus tree of the MrBayes analysis of the Primulacaeae dataset under the optimal, fully partitioned model. Posterior probability is indicated to the right of nodes, scale bar indicates expected number of substitutions per site. First page contains the /Primula clade, with clades /Soldanella and /Androsace collapsed; the /Primula clade is collapsed on the second page. Note that the clades /Primula, /Soldanella and /Androsace received 100% posterior probability, justifying to constrain them as monophyletic in the BEAST analyses. (B) Maximum clade credibility chronogram with median node heights based on the BEAST dating analysis using the uncorrelated relaxed lognormal (UCLN) relaxed-clock model. Posterior probability is indicated at nodes, scale axis indicates divergence times in millions of years. The interval of 95% highest posterior density of divergence times is given by bars at nodes with >0.95 posterior probability. First page contains the /Primula clade, with the clades /Soldanella and /Androsace collapsed. The /Primula clade is collapsed on the second page. (C) Maximum clade credibility chronogram based on the BEAST dating analysis using the uncorrelated relaxed exponential (UCEXP) relaxed-clock model, annotated as described for Fig. S1B.

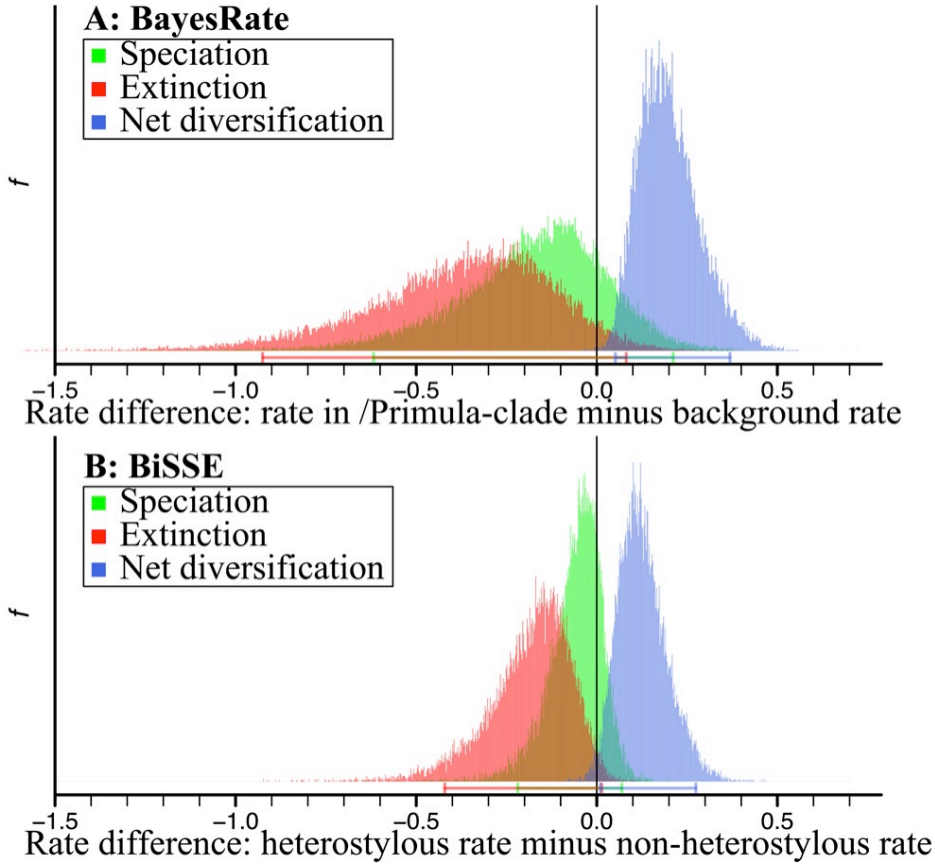

Fig. S2. Posterior distributions of differences in rates of extinction (red), speciation (green), and net diversification (blue) between (A) heterostylous and non-heterostylous clades using BayesRate and (B) heterostylous and non-heterostylous lineages using Bayesian BiSSE, based on trees from the dating analysis with uncorrelated exponential relaxed-clock model (UCEXP). Lines of corresponding colours below the distributions denote the 95% intervals of highest posterior density; intervals that include zero indicate no significant difference in rate. Both types of analyses indicate no significant difference in speciation rates between heterostylous and non-heterostylous lineages, but significantly lower extinction rates (or marginally so), hence, higher diversification rates of heterostylous lineages.

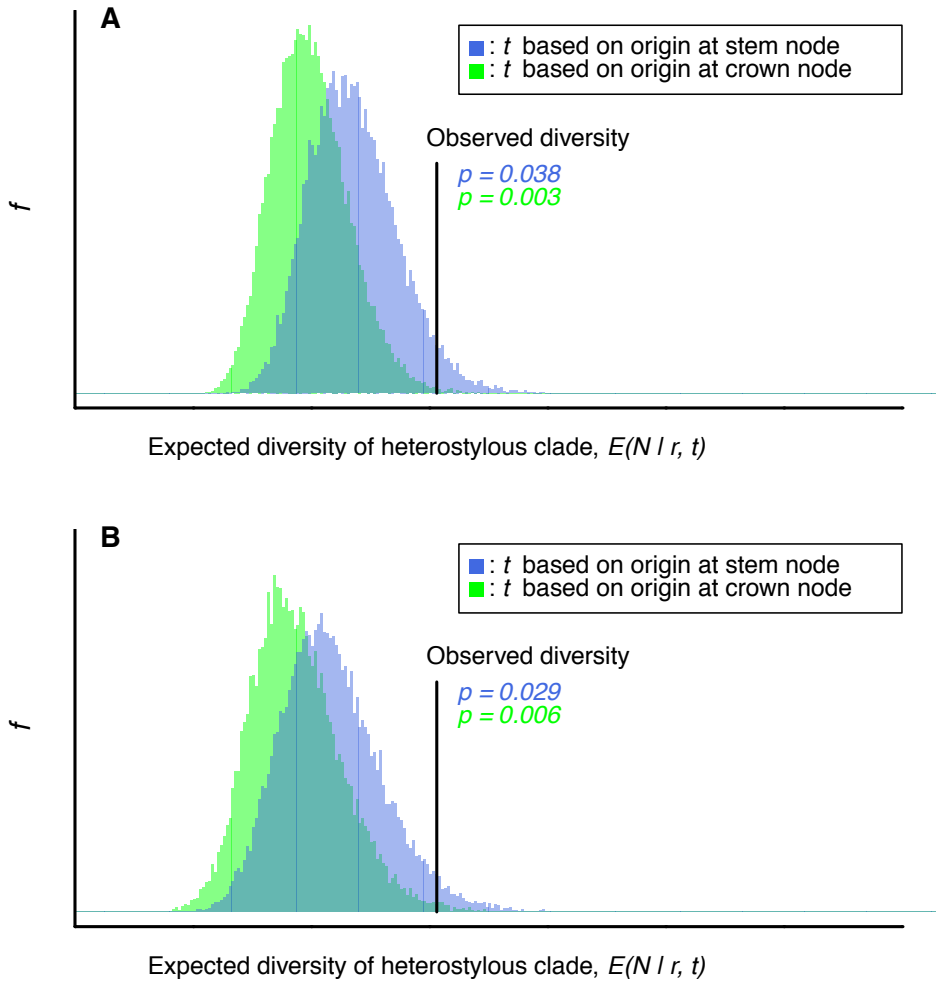

Fig. S3. Results of the CVPDD analyses. Frequency distributions of species diversity in the /Primula clade expected from the background diversification rate, *r* (i.e., the rate at which /Androsace + /Soldanella diversify) and the timing of the origin of heterostyly, *t*, corresponding to stem or crown node ages of the /Primula clade (nodes b and c in Fig. 2, respectively). The parameters *t* and *r* were estimated in separate BEAST runs that employed (A) a UCLN relaxed clock model or (B) a UCEXP relaxed clock model. See Text S1 for further details.

Table S1. Ancestral state reconstructions of heterostyly in Primulaceae for five nodes of interest. Presence (1) or absence (0) of heterostyly nodes of interest under maximum parsimony (MP), the median probability of the node being heterostylous under maximum likelihood (ML) and Bayesian (BI) inference ± the interquartile range across 100 trees from the posterior distribution, and BayesFactor (BF) support for ancestral states, where positive and negative values indicate support for presence and absence of heterostyly, respectively. ML analyses accounted for state-dependent diversification (see Text S1).

Dating analysis	Node of interest[1]	MP[2]	Scheme 1			Scheme 2			Scheme 3			Scheme 4		
			ML	BI	BF[3]	ML	BI	BF[3]	ML	BI	BF[3]	ML	BI	BF[3]
UCEXP	a	0	0.265± 0.168	0.478 ± 0.244	-0.50	0.390± 0.250	0.534 ± 0.224	0.20	0.506± 0.281	0.553 ± 0.196	0.30	1.000± 0.304	0.684 ± 0.304	1.81
	b	0	0.375± 0.221	0.854 ± 0.145	0.33	0.487± 0.276	0.872 ± 0.119	0.64	0.584± 0.278	0.87 ± 0.115	1.63	1.000± 0.250	0.934 ± 0.105	2.16
	c	1	0.977± 0.035	0.999 ± 0.003	8.05	0.982± 0.029	0.999 ± 0.003	8.38	0.985± 0.024	0.997 ± 0.009	8.04	1.000± 0.001	1.000 ± 0.001	10.08
	d	0	0.060± 0.062	0.154 ± 0.133	-2.66	0.097± 0.095	0.214 ± 0.14	-1.54	0.150± 0.119	0.218 ± 0.151	-1.93	0.022± 0.026	0.036 ± 0.048	-5.3
	e	0	0.015± 0.028	0.045 ± 0.067	-4.53	0.027± 0.042	0.067 ± 0.065	-4.09	0.047± 0.066	0.081 ± 0.084	-3.90	0.053± 0.077	0.056 ± 0.065	-3.17
UCLN	a	0	0.189± 0.072	0.48 ± 0.231	-0.49	0.282± 0.108	0.539 ± 0.205	0.09	0.382± 0.136	0.544 ± 0.178	0.28	1.000± 0.655	0.704 ± 0.272	1.61
	b	0	0.280± 0.091	0.884 ± 0.113	1.27	0.383± 0.130	0.898 ± 0.106	1.55	0.493± 0.170	0.88 ± 0.118	2.21	1.000± 0.550	0.950 ± 0.075	2.97
	c	1	0.970± 0.039	0.998 ± 0.005	7.60	0.977± 0.032	0.997 ± 0.008	7.44	0.981± 0.021	0.993 ± 0.02	7.25	1.000± 0.001	1.000 ± 0.001	10.63
	d	0	0.041± 0.027	0.191 ± 0.126	-2.25	0.072± 0.045	0.241 ± 0.130	-1.68	0.111± 0.068	0.268 ± 0.122	-1.67	0.020± 0.017	0.058 ± 0.048	-4.86
	e	0	0.007± 0.006	0.048 ± 0.05	-4.95	0.014± 0.014	0.083 ± 0.072	-3.88	0.026± 0.025	0.13 ± 0.098	-3.25	0.034± 0.035	0.069 ± 0.058	-3.54

Notes:

1: Nodes of interest are indicated in Fig. 2, and represent: a, the root node; b, stem lineage of /Primula; c, crown node of /Primula; d, crown node of /Soldanella; e, crown node of /Androsace.

2: Parsimony results are identical across trees and character coding schemes.

3: BF values greater than 2 (or smaller than -2) indicate "Positive support", values greater than 6 (or smaller than -6) indicate "Strong support", and values greater than 10 (or smaller than -10) indicate "Very strong support [52]

Table S2. Results of analyses to detect shifts in diversification rate using (A) MEDUSA and (B) SymmeTREE. (A) Results of MEDUSA analyses, indicating the dating analysis on which the input tree was based, diversification model fitted (base model: no rate shifts; optimal model: including rate shifts), number of the nodes where the diversification rate was inferred to change, the Maximum Likelihood estimates of *r* (net diversification) and ε (relative extinction) for the tree partition, the fit of the model to the data based on AICc value, and the magnitude of the change in diversification rate along the /Primula stem lineage (between nodes b and c; see Fig. 2 of the main text). (B) Results of SymmeTREE analyses, indicating the nodes where the difference in net diversification rate between the two descending daughter lineages was significant or marginally significant, the value of the shift statistics Δ1 and Δ2 and associated P-values. Results of SymmeTREE analyses on trees obtained under both dating analyses were identical. Nodes are numbered according to standard NEXUS tree representation.

A

Dating analysis	Diversification model	Node number	*r*	ε	AICc	Increase along /Primula stem lineage?
UCEXP	Base model	NA	0.22	0.06	1312.615	NA
	Optimal model	266	0.11	0.40	1292.124	2.18-fold[2]
		503	0.59	0.00		
		268[1]	0.26	0.00		
		327	0.71	0.00		
UCLN	Base model	NA	0.19	0.41	1312.615	NA
	Optimal model	266	0.08	0.52	1199.898	3.46-fold[2]
		474	0.73	0.00		
		268[1]	0.28	0.00		
		280	1.03	0.12		

B

Node number	Shift statistic Δ1	$P_{\Delta 1}$	Shift statistic Δ2	$P_{\Delta 2}$
267[3]	1.973	0.063	1.786	0.08
285	2.752	0.047	2.485	0.06
335	3.039	0.024	2.773	0.027
338	1.682	0.086	1.576	0.099
345	2.315	0.077	2.079	0.099
438	2.534	0.038	2.303	0.045
471	2.56	0.056	2.303	0.065
473	2.537	0.058	2.303	0.075

Notes:

1: Node 268 represents the most recent common ancestor of all heterostylous species in the /Primula clade (i.e. of >99% of all heterostylous species). A rate shift at this node was also recovered in all trees in a sample of 100 trees from the posterior distribution.

2: Calculated using *r* from position 266 (root) and 268 (/Primula crown node)

3: SymmeTREE (B) identifies nodes of which the two daughter clades have significantly different diversification rates, whereas MEDUSA (A) identifies the nodes at which the diversification rate has changed. Hence, the nodes identified by MEDUSA (node 267) and SymmeTREE (node 268) point to a diversification rate shift along the same branch, i.e. b-c in Fig. 2 (main text).

Table S3. Model fitting and parameterization of BayesRate (A), BiSSE (B-E), and MuSSE (F) models for heterostylous and non-heterostylous lineages of family-wide and /Primula-wide datasets. Results indicate congruence between models (BiSSE vs. BayesRate vs. MuSSE), and contrasting net effects of heterostyly across time scales (Family-wide vs. /Primula clade). Indicated are median rates of speciation, λ, and extinction, μ, of heterostylous (subscript 1) and non-heterostylous (subscript 0) species, their net diversification rates, r, and the difference in their net diversification rates [$(\lambda_1-\mu_1)$ - $(\lambda_0-\mu_0)$, i.e., positive values indicate that heterostylous species diversify at a higher rate], estimated ± interquartile range over 100 trees from the posterior distribution of the UCLN and UCEXP dating analyses, for all diversification models considered. Models are sorted by AIC-weights, so that the best supported model for each data set is at the top and the worst at the bottom. Bold-faced models are best supported by BayesFactors (BayesRate) or AIC-weight (other analyses). Constrained parameters were forced to be identical between heterostylous and non-heterostylous lineages (BiSSE, MuSSE) or identical between /Primula and /Soldanella+/Androsace (BayesRate); free parameters were estimated separately for tree partitions.

Table S3A. Family-wide analysis using BayesRate.

Dating analysis	Model specification			Model support					Model parameterization								Net effect of heterosyly
	Speciation rate	Extinction rate	Transition rate	No. parameters	Log likelihood[1]	ΔAIC	AIC-weight[2]	Bayes-Factor[3]	λ_0	λ_1	μ_0	μ_1	q_{01}	q_{10}	$r_0 = \lambda_0 - \mu_0$	$r_1 = \lambda_1 - \mu_1$	$\Delta r = r_1 - r_0$
UCLN	**Constrained**	**Free**	-	**3**	**-663.06**	-	-	**0**	**0.772 ± 0.306**	**0.772 ± 0.306**	**0.679 ± 0.295**	**0.374 ± 0.231**	-	-	**0.083 ± 0.056**	**0.383 ± 0.154**	**0.293 ± 0.139**
	Constrained	Constrained	-	2	-674.63	-	-	-23.15	0.619 ± 0.308	0.619 ± 0.308	0.396 ± 0.246	0.396 ± 0.246	-	-	0.216 ± 0.1	0.216 ± 0.1	0 ± 0
	Free	Constrained	-	3	-709.96	-	-	-93.8	0.702 ± 0.296	0.92 ± 0.363	0.587 ± 0.28	0.587 ± 0.28	-	-	0.105 ± 0.061	0.325 ± 0.128	0.211 ± 0.104
	Free	Free	-	4	-717.91	-	-	-109.7	1.021 ± 0.482	0.664 ± 0.273	0.932 ± 0.475	0.234 ± 0.214	-	-	0.083 ± 0.053	0.412 ± 0.164	0.321 ± 0.148
UCEXP	**Constrained**	**Free**	-	**3**	**-727.69**	-	-	**0**	**0.563 ± 0.277**	**0.563 ± 0.277**	**0.441 ± 0.249**	**0.258 ± 0.197**	-	-	**0.116 ± 0.073**	**0.302 ± 0.135**	**0.178 ± 0.103**
	Constrained	Constrained	-	2	-736.48	-	-	-17.58	0.619 ± 0.308	0.619 ± 0.308	0.396 ± 0.246	0.396 ± 0.246	-	-	0.216 ± 0.1	0.216 ± 0.1	0 ± 0
	Free	Constrained	-	3	-791.99	-	-	-128.61	0.514 ± 0.259	0.64 ± 0.312	0.367 ± 0.226	0.367 ± 0.226	-	-	0.141 ± 0.083	0.269 ± 0.119	0.124 ± 0.079
	Free	Free	-	4	-794.57	-	-	-133.77	0.682 ± 0.381	0.516 ± 0.264	0.558 ± 0.361	0.193 ± 0.193	-	-	0.114 ± 0.074	0.312 ± 0.137	0.191 ± 0.113

Table S3B. Family-wide analysis using BiSSE.

Dating analysis	Model specification			Model support					Model parameterization								Net effect of heterosyly
	Speciation rate	Extinction rate	Transition rate	No. parameters	Log likelihood[1]	ΔAIC	AIC-weight[2]	Bayes-Factor[3]	λ_0	λ_1	μ_0	μ_1	q_{01}	q_{10}	$r_0 = \lambda_0 - \mu_0$	$r_1 = \lambda_1 - \mu_1$	$\Delta r = r_1 - r_0$
UCLN	**Free**	**Free**	**Free**	**6**	**-698 ± 84**	**0.00**	**0.56**	-	**0.431 ± 0.14**	**0.315 ± 0.113**	**0.355 ± 0.138**	**0 ± 0**	**0.005 ± 0.002**	**0.061 ± 0.022**	**0.072 ± 0.023**	**0.315 ± 0.113**	**0.243 ± 0.095**
	Constrained	**Free**	**Free**	**5**	**-699 ± 84**	**0.48**	**0.44**	-	**0.328 ± 0.111**	**0.328 ± 0.111**	**0.244 ± 0.096**	**0 ± 0**	**0.007 ± 0.002**	**0.055 ± 0.021**	**0.083 ± 0.029**	**0.328 ± 0.111**	**0.244 ± 0.096**
	Constrained	Free	Constrained	5	-706 ± 84	13.73	0	-	0.32 ± 0.112	0.32 ± 0.112	0.186 ± 0.075	0.035 ± 0.04	0.028 ± 0.009	0.028 ± 0.009	0.134 ± 0.043	0.282 ± 0.1	0.151 ± 0.054
	Free	Constrained	Free	5	-706 ± 84	14.63	0	-	0.279 ± 0.094	0.38 ± 0.14	0.136 ± 0.07	0.136 ± 0.07	0.012 ± 0.004	0.041 ± 0.015	0.141 ± 0.05	0.241 ± 0.083	0.096 ± 0.048
	Free	Free	Constrained	6	-706 ± 84	15.64	0	-	0.329 ± 0.103	0.316 ± 0.115	0.194 ± 0.088	0.034 ± 0.049	0.028 ± 0.009	0.028 ± 0.009	-0.158 ± 0.053	0.135 ± 0.042	0.282 ± 0.098
	Free	Constrained	Constrained	5	-708 ± 84	17.16	0	-	0.285 ± 0.096	0.366 ± 0.136	0.125 ± 0.069	0.125 ± 0.069	0.03 ± 0.01	0.03 ± 0.01	0.157 ± 0.054	0.237 ± 0.083	0.078 ± 0.033
	Constrained	Constrained	Free	4	-708 ± 83	19.20	0	-	0.339 ± 0.127	0.339 ± 0.127	0.137 ± 0.078	0.137 ± 0.078	0.015 ± 0.008	0.039 ± 0.014	0.197 ± 0.065	0.197 ± 0.065	0 ± 0
	Constrained	Constrained	Constrained	4	-710 ± 84	19.00	0	-	0.339 ± 0.127	0.339 ± 0.127	0.137 ± 0.078	0.137 ± 0.078	0.032 ± 0.011	0.032 ± 0.011	0.197 ± 0.065	0.197 ± 0.065	0 ± 0

UCEXP	**Constrained**	**Free**	**Free**	**5**	**-755 ± 115**	**0.00**	**0.43**	**-**	**0.249 ± 0.107**	**0.249 ± 0.107**	**0.133 ± 0.068**	**0 ± 0**	**0.007 ± 0.004**	**0.039 ± 0.02**	**0.108 ± 0.05**	**0.249 ± 0.107**	**0.133 ± 0.068**
	Free	**Free**	**Free**	**6**	**-754 ± 115**	**0.86**	**0.31**	**-**	**0.288 ± 0.13**	**0.245 ± 0.1**	**0.19 ± 0.106**	**0 ± 0**	**0.006 ± 0.003**	**0.041 ± 0.021**	**0.098 ± 0.046**	**0.245 ± 0.1**	**0.138 ± 0.069**
	Constrained	Free	Constrained	4	-759 ± 118	5.00	0.05	-	0.239 ± 0.109	0.239 ± 0.109	0.082 ± 0.046	0 ± 0.01	0.024 ± 0.012	0.024 ± 0.012	0.152 ± 0.066	0.231 ± 0.103	0.076 ± 0.038
	Constrained	Constrained	Constrained	3	-761 ± 118	6.22	0.02	-	0.234 ± 0.11	0.234 ± 0.11	0.015 ± 0.05	0.015 ± 0.05	0.025 ± 0.011	0.025 ± 0.011	0.203 ± 0.081	0.203 ± 0.081	0 ± 0
	Constrained	Constrained	Free	4	-760 ± 117	6.51	0.02	-	0.234 ± 0.11	0.234 ± 0.11	0.015 ± 0.05	0.015 ± 0.05	0.013 ± 0.009	0.03 ± 0.013	0.203 ± 0.081	0.203 ± 0.081	0 ± 0
	Free	Free	Constrained	5	-759 ± 117	6.65	0.02	-	0.237 ± 0.109	0.241 ± 0.101	0.088 ± 0.065	0 ± 0	0.025 ± 0.011	0.025 ± 0.011	-0.082 ± 0.057	0.151 ± 0.065	0.229 ± 0.095
	Free	Constrained	Free	5	-759 ± 116	6.33	0.02	-	0.204 ± 0.101	0.251 ± 0.124	0.023 ± 0.052	0.023 ± 0.052	0.012 ± 0.007	0.03 ± 0.014	0.173 ± 0.082	0.216 ± 0.077	0.042 ± 0.036
	Free	Constrained	Constrained	4	-760 ± 117	7.01	0.02	-	0.206 ± 0.102	0.248 ± 0.118	0.017 ± 0.048	0.017 ± 0.048	0.025 ± 0.011	0.025 ± 0.011	0.18 ± 0.082	0.216 ± 0.077	0.033 ± 0.034

Table S3C. /Primula analysis using BiSSE.

Dating analysis	Model specification			Model support					Model parameterization								Net effect of heterosyly
	Speciation rate	Extinction rate	Transition rate	No. para-meters	Log likelihood[1]	ΔAIC	AIC-weight[2]	Bayes-Factor[3]	λ_0	λ_1	μ_0	μ_1	q_{01}	q_{10}	$r_0 = \lambda_0 - \mu_0$	$r_1 = \lambda_1 - \mu_1$	$\Delta r = r_1 - r_0$
UCLN	**Free**	**Constrained**	**Free**	**5**	**-486 ± 69**	**0.00**	**0.72**	**-**	**0.639 ± 0.263**	**0.188 ± 0.076**	**0 ± 0**	**0 ± 0**	**0.748 ± 0.401**	**0.099 ± 0.076**	**0.639 ± 0.263**	**0.186 ± 0.076**	**-0.433 ± 0.231**
	Free	**Free**	**Free**	**6**	**-486 ± 69**	**2.00**	**0.27**	**-**	**0.639 ± 0.264**	**0.188 ± 0.076**	**0 ± 0**	**0 ± 0**	**0.749 ± 0.4**	**0.099 ± 0.074**	**0.639 ± 0.264**	**0.186 ± 0.075**	**-0.435 ± 0.219**
	Constrained	Constrained	Free	4	-491 ± 69	9.49	0.01	-	0.302 ± 0.108	0.302 ± 0.108	0 ± 0	0 ± 0	0.303 ± 0.105	0.05 ± 0.018	0.302 ± 0.108	0.302 ± 0.108	0 ± 0
	Constrained	Free	Free	5	-491 ± 69	11.49	0	-	0.302 ± 0.108	0.302 ± 0.108	0 ± 0	0 ± 0	0.302 ± 0.105	0.05 ± 0.018	0.302 ± 0.108	0.302 ± 0.108	0 ± 0
	Free	Free	Constrained	6	-494 ± 63	19.84	0	-	0.573 ± 0.208	0.313 ± 0.106	0.532 ± 0.212	0 ± 0	0.076 ± 0.025	0.076 ± 0.025	-0.532 ± 0.212	0.037 ± 0.027	0.313 ± 0.106
	Constrained	Free	Constrained	5	-495 ± 63	20.88	0	-	0.324 ± 0.113	0.324 ± 0.113	0.314 ± 0.114	0 ± 0	0.071 ± 0.024	0.071 ± 0.024	0.014 ± 0.031	0.324 ± 0.113	0.314 ± 0.114
	Constrained	Constrained	Constrained	4	-498 ± 62	24.27	0	-	0.303 ± 0.103	0.303 ± 0.103	0 ± 0	0 ± 0	0.042 ± 0.014	0.042 ± 0.014	0.303 ± 0.103	0.303 ± 0.103	0 ± 0
	Free	Constrained	Constrained	5	-498 ± 62	25.32	0	-	0.37 ± 0.131	0.297 ± 0.099	0 ± 0	0 ± 0	0.041 ± 0.014	0.041 ± 0.014	0.37 ± 0.131	0.297 ± 0.099	-0.07 ± 0.056
UCEXP	**Free**	**Constrained**	**Free**	**5**	**-535 ± 82**	**0.00**	**0.39**	**-**	**0.338 ± 0.136**	**0.209 ± 0.094**	**0 ± 0**	**0 ± 0**	**0.285 ± 0.142**	**0.041 ± 0.019**	**0.338 ± 0.136**	**0.209 ± 0.094**	**-0.118 ± 0.108**
	Constrained	**Constrained**	**Free**	**4**	**-536 ± 80**	**0.31**	**0.33**	**-**	**0.237 ± 0.099**	**0.237 ± 0.099**	**0 ± 0**	**0 ± 0**	**0.227 ± 0.107**	**0.039 ± 0.017**	**0.237 ± 0.099**	**0.237 ± 0.099**	**0 ± 0**
	Free	Free	Free	6	-535 ± 82	2.00	0.14	-	0.338 ± 0.138	0.209 ± 0.096	0 ± 0	0 ± 0	0.291 ± 0.147	0.041 ± 0.019	0.338 ± 0.138	0.209 ± 0.094	-0.12 ± 0.111
	Constrained	Free	Free	5	-536 ± 80	2.31	0.12	-	0.237 ± 0.102	0.237 ± 0.102	0 ± 0	0 ± 0	0.228 ± 0.107	0.039 ± 0.017	0.237 ± 0.102	0.237 ± 0.099	0 ± 0
	Free	Free	Constrained	5	-540 ± 81	11.33	0	-	0.403 ± 0.196	0.246 ± 0.1	0.364 ± 0.199	0 ± 0	0.056 ± 0.029	0.056 ± 0.029	-0.364 ± 0.199	0.035 ± 0.044	0.246 ± 0.1
	Constrained	Free	Constrained	4	-541 ± 78	11.44	0	-	0.251 ± 0.107	0.251 ± 0.107	0.229 ± 0.119	0 ± 0	0.052 ± 0.024	0.052 ± 0.024	0.014 ± 0.052	0.251 ± 0.107	0.229 ± 0.119
	Constrained	Constrained	Constrained	3	-544 ± 77	13.78	0	-	0.237 ± 0.099	0.237 ± 0.099	0 ± 0	0 ± 0	0.033 ± 0.014	0.033 ± 0.014	0.237 ± 0.099	0.237 ± 0.099	0 ± 0
	Free	Constrained	Constrained	4	-544 ± 78	15.39	0	-	0.274 ± 0.13	0.236 ± 0.092	0 ± 0	0 ± 0	0.033 ± 0.013	0.033 ± 0.013	0.274 ± 0.13	0.235 ± 0.092	-0.04 ± 0.048

Table S3D. Family-wide analysis using BiSSE, excluding polyploids. Note caveats and details that are discussed in text S1.

Dating analysis	Model specification			Model support					Model parameterization								Net effect of heterosyly
	Speciation rate	Extinction rate	Transition rate	No. parameters	Log likelihood[1]	ΔAIC	AIC-weight[2]	Bayes-Factor[3]	λ_0	λ_1	μ_0	μ_1	q_{01}	q_{10}	$r_0 = \lambda_0 - \mu_0$	$r_1 = \lambda_1 - \mu_1$	$\Delta r = r_1 - r_0$
UCLN	**Constrained**	**Free**	**Free**	**5**	**-512 ± 60**	**0**	**0.66**	-	**0.564 ± 0.187**	**0.564 ± 0.187**	**0.468 ± 0.161**	**0 ± 0.050**	**0.005 ± 0.002**	**0.081 ± 0.030**	**0.099 ± 0.034**	**0.542 ± 0.21**	**0.441 ± 0.168**
	Free	**Free**	**Free**	**6**	**-512 ± 60**	**1.85**	**0.27**	-	**0.630 ± 0.231**	**0.559 ± 0.199**	**0.540 ± 0.217**	**0 ± 0.027**	**0.004 ± 0.002**	**0.084 ± 0.032**	**0.094 ± 0.036**	**0.545 ± 0.203**	**0.450 ± 0.167**
	Free	Constrained	Free	5	-514 ± 60	5.27	0.05	-	0.414 ± 0.188	0.719 ± 0.269	0.292 ± 0.152	0.292 ± 0.152	0.006 ± 0.004	0.059 ± 0.021	0.124 ± 0.043	0.428 ± 0.155	0.306 ± 0.111
	Constrained	Constrained	Free	4	-527 ± 59	29.52	0	-	0.817 ± 0.29	0.817 ± 0.29	0.603 ± 0.252	0.603 ± 0.252	0.005 ± 0.003	0.039 ± 0.015	0.218 ± 0.071	0.218 ± 0.071	0 ± 0
UCEXP	**Constrained**	**Free**	**Free**	**5**	**-547 ± 76**	**0**	**0.55**	-	**0.499 ± 0.247**	**0.499 ± 0.247**	**0.389 ± 0.196**	**0.140 ± 0.105**	**0.004 ± 0.003**	**0.051 ± 0.021**	**0.112 ± 0.045**	**0.348 ± 0.145**	**0.236 ± 0.127**
	Free	**Free**	**Free**	**6**	**-546 ± 76**	**1.63**	**0.25**	-	**0.575 ± 0.267**	**0.487 ± 0.230**	**0.461 ± 0.241**	**0.105 ± 0.119**	**0.004 ± 0.002**	**0.056 ± 0.023**	**0.103 ± 0.038**	**0.364 ± 0.149**	**0.250 ± 0.124**
	Free	Constrained	Free	5	-549 ± 77	2.21	0.19	-	0.406 ± 0.207	0.583 ± 0.285	0.27 ± 0.154	0.27 ± 0.154	0.005 ± 0.004	0.04 ± 0.018	0.132 ± 0.054	0.308 ± 0.114	0.172 ± 0.085
	Constrained	Constrained	Free	4	-558 ± 80	13.37	0	-	0.586 ± 0.31	0.586 ± 0.31	0.369 ± 0.224	0.369 ± 0.224	0.005 ± 0.004	0.03 ± 0.012	0.217 ± 0.092	0.217 ± 0.092	0 ± 0

Table S3E. /Primula analysis using BiSSE, excluding polyploids. Note caveats and details that are discussed in text S1.

Dating analysis	Model specification			Model support					Model parameterization								Net effect of heterosyly
	Speciation rate	Extinction rate	Transition rate	No. parameters	Log likelihood[1]	ΔAIC	AIC-weight[2]	Bayes-Factor[3]	λ_0	λ_1	μ_0	μ_1	q_{01}	q_{10}	$r_0 = \lambda_0 - \mu_0$	$r_1 = \lambda_1 - \mu_1$	$\Delta r = r_1 - r_0$
UCLN	**Free**	**Constrained**	**Free**	**5**	**-392 ± 50**	**0**	**0.73**	-	**0.708 ± 0.333**	**0.177 ± 0.070**	**0 ± 0**	**0 ± 0**	**0.996 ± 0.446**	**0.163 ± 0.074**	**0.706 ± 0.333**	**0.177 ± 0.071**	**-0.532 ± 0.232**
	Free	**Free**	**Free**	**6**	**-392 ± 50**	**2**	**0.27**	-	**0.709 ± 0.327**	**0.177 ± 0.070**	**0 ± 0**	**0 ± 0**	**0.997 ± 0.431**	**0.163 ± 0.072**	**0.709 ± 0.327**	**0.176 ± 0.067**	**-0.542 ± 0.231**
	Constrained	Constrained	Free	4	-399 ± 50	12.13	0	-	0.304 ± 0.103	0.304 ± 0.103	0 ± 0	0 ± 0	0.382 ± 0.159	0.075 ± 0.031	0.304 ± 0.103	0.304 ± 0.103	0 ± 0
	Constrained	Free	Free	5	-399 ± 50	14.13	0	-	0.304 ± 0.103	0.304 ± 0.103	0 ± 0	0 ± 0	0.382 ± 0.161	0.075 ± 0.031	0.304 ± 0.108	0.304 ± 0.103	0 ± 0
UCEXP	**Constrained**	**Constrained**	**Free**	**4**	**-434 ± 62**	**0**	**0.44**	-	**0.243 ± 0.099**	**0.243 ± 0.099**	**0 ± 0**	**0 ± 0**	**0.276 ± 0.150**	**0.056 ± 0.029**	**0.243 ± 0.097**	**0.243 ± 0.097**	**0 ± 0**
	Free	**Constrained**	**Free**	**5**	**-432 ± 64**	**0.92**	**0.28**	-	**0.343 ± 0.200**	**0.206 ± 0.110**	**0 ± 0**	**0 ± 0**	**0.406 ± 0.329**	**0.073 ± 0.042**	**0.340 ± 0.191**	**0.206 ± 0.108**	**-0.112 ± 0.258**
	Constrained	Free	Free	5	-434 ± 62	2	0.17	-	0.244 ± 0.099	0.244 ± 0.099	0 ± 0	0 ± 0	0.263 ± 0.154	0.056 ± 0.030	0.233 ± 0.097	0.244 ± 0.097	0 ± 0
	Free	Free	Free	6	-432 ± 64	2.88	0.11	-	0.347 ± 0.191	0.206 ± 0.111	0 ± 0	0 ± 0	0.406 ± 0.335	0.073 ± 0.041	0.339 ± 0.199	0.203 ± 0.108	-0.116 ± 0.263

Table S3F. Family-wide analysis using MuSSE, assigning separate states to diploids (states 1, 2) and polyploids (states 3, 4) for heterostylous (states 2, 4) and non-heterostylous (states 1, 3) species. Note caveats that are discussed in text S1.

	Model parameterization																Net diversification rate				Net effect of heterostyly	
Dating analysis	λ_1	λ_2	λ_3	λ_4	μ_1	μ_2	μ_3	μ_4	q_{12}	q_{13}	q_{21}	q_{24}	q_{31}	q_{34}	q_{42}	q_{43}	$r_1 = \lambda_1 - \mu_1$	$r_2 = \lambda_2 - \mu_2$	$r_3 = \lambda_3 - \mu_3$	$r_4 = \lambda_4 - \mu_4$	*among diploids*	*among poly-ploids*
UCLN	0.147 ± 0.053	0.286 ± 0.152	0.809 ± 0.321	0.440 ± 0.221	0.004 ± 0	0 ± 0	0.691 ± 0.342	0.142 ± 0.225	0.001 ± 0	0.101 ± 0.044	0.053 ± 0.018	0.038 ± 0.015	0.013 ± 0.007	0.033 ± 0.015	0.238 ± 0.299	0.078 ± 0.037	0.143 ± 0.054	0.286 ± 0.152	0.118 ± 0.046	0.299 ± 0.397	0.143 ± 0.097	0.181 ± 0.228
UCEXP	0.145 ± 0.066	0.241 ± 0.106	0.473 ± 0.230	0.278 ± 0.141	0.008 ± 0	0 ± 0	0.301 ± 0.230	0.066 ± 0.115	0.018 ± 0.031	0.083 ± 0.050	0.041 ± 0.016	0.023 ± 0.010	0.022 ± 0.021	0.016 ± 0.019	0.090 ± 0.090	0.049 ± 0.042	0.137 ± 0.064	0.241 ± 0.106	0.172 ± 0.100	0.213 ± 0.140	0.103 ± 0.058	0.041 ± 0.13

Notes:

1: Log likelihoods are marginal likelihoods across the sample of trees from the posterior for BayesRate models, and median values ± interquartile range of maximum-likelihood estimates across the trees sampled from the posterior.

2: AIC-weights are roughly interpreted as the approximate probability that a model is the best-fitting one among the set of models considered.

3: BayesFactors are expressed relative to the model of highest marginal likelihood. Thus, the more negative the BayesFactor, the more strongly supported the best model is over that model. BayesFactor < -10 are interpreted as "Very strong support" [52]

Table S4. Number of known and sampled species in Primulaceae, indicating the phylogenetic (clade) and taxonomic (genus and section) affinity, the number of species included in recent revisions, the estimated number of species including recently described species, the number of sampled species, the total number of species that are heterostylous, the number of sampled heterostylous species, the numbers of sampled species divided by the total number of species, and the number of sampled heterostylous species divided by the total number of heterostylous species. Note that the proportion of known species that are sampled in this study is similar among the three main clades and that the proportion of sampled species that are heterostylous is similar to the proportion of known species that are heterostylous.

Clade	**Genus**	**Section**	Number of species in revisions and Flora of China[1]	Estimated total number of species[2]	Number of sampled species	Total number of heterostylous species[3]	Number of sampled heterostylous species[4]	Fraction of sampled species among all species	Fraction of sampled heterostylous species among all heterostylous species
/Androsace	*Androsace*	*Aizoidium*	3	3	1	0	0	0.33	NA
/Androsace	*Androsace*	*Andraspis*	17	17	11	0	0	0.65	NA
/Androsace	*Androsace*	*Aretia*	21	22	27	0	0	1.23	NA
/Androsace	*Androsace*	*Chamaejasme*	77	78	15	0	0	0.19	NA
/Androsace	*Androsace*	*Pseudoprimula*	24	24	3	0	0	0.13	NA
/Androsace	*Androsace*	*"Vitaliana"*	1	1	1	1	1	1.00	1.00
/Androsace	*Douglasia*		9	9	7	0	0	0.78	NA
/Androsace	*Pomatosace*		1	1	1	0	0	1.00	NA
/Primula	*Cortusa*		13	8	3	0	0	0.38	NA
/Primula	*Dionysia*		49	49	9	47	9	0.18	0.19
/Primula	*Dodecatheon*		17	17	8	0	0	0.47	NA
/Primula	*Primula*	*Aleuritia*	27	38	16	28	11	0.42	0.39
/Primula	*Primula*	*Amethystina*	8	8	2	8	2	0.25	0.25
/Primula	*Primula*	*Armerina*	14	14	6	10	5	0.43	0.50
/Primula	*Primula*	*Auganthus*	2	2	2	2	2	1.00	1.00
/Primula	*Primula*	*Auricula*	22	22	9	22	9	0.41	0.41
/Primula	*Primula*	*Bullatae*	7	7	2	7	2	0.29	0.29
/Primula	*Primula*	*Capitatae*	2	2	2	2	2	1.00	1.00
/Primula	*Primula*	*Carolinella*	9	11	5	7	4	0.45	0.57
/Primula	*Primula*	*Chartacea*	5	8	1	7	1	0.13	0.14
/Primula	*Primula*	*Cordifoliae*	7	8	3	6	3	0.38	0.50
/Primula	*Primula*	*Cortusoides*	22	27	9	24	7	0.33	0.29
/Primula	*Primula*	*Crystallophlomis*	45	53	13	49	12	0.25	0.24
/Primula	*Primula*	*Cuneifolia*	2	2	3	1	2	1.50	2.00
/Primula	*Primula*	*Davidii*	17	20	3	18	3	0.15	0.17
/Primula	*Primula*	*Denticulata*	12	14	5	14	5	0.36	0.36
/Primula	*Primula*	*Dryadifolia*	4	4	1	4	1	0.25	0.25
/Primula	*Primula*	*Fedtschenkoana*	1	1	1	1	1	1.00	1.00
/Primula	*Primula*	*Glabra*	3	3	1	2	1	0.33	0.50
/Primula	*Primula*	*Malvacea*	5	6	4	6	4	0.67	0.67
/Primula	*Primula*	*Minutissimae*	23	24	7	16	5	0.29	0.31
/Primula	*Primula*	*Monocarpicae*	13	14	4	14	4	0.29	0.29
/Primula	*Primula*	*Muscarioides*	19	20	10	15	7	0.50	0.47
/Primula	*Primula*	*Obconicolisteri*	16	16	4	9	2	0.25	0.22

/Primula	*Primula*	*Oreophlomis*	8	8	5	8	5	0.63	0.63
/Primula	*Primula*	*Parryi*	5	5	6	5	6	1.20	1.20
/Primula	*Primula*	*Petiolares*	28	39	9	37	9	0.23	0.24
/Primula	*Primula*	*Pinnatae*	4	4	2	2	1	0.50	0.50
/Primula	*Primula*	*Primula*	6	6	4	6	4	0.67	0.67
/Primula	*Primula*	*Proliferae*	19	24	10	16	5	0.42	0.31
/Primula	*Primula*	*Pulchella*	14	14	1	14	1	0.07	0.07
/Primula	*Primula*	*Pycnoloba*	1	1	1	1	1	1.00	1.00
/Primula	*Primula*	*Reinii*	4	4	1	4	1	0.25	0.25
/Primula	*Primula*	*Sikkimensis*	9	9	4	8	4	0.44	0.50
/Primula	*Primula*	*Soldanelloides*	18	18	2	17	2	0.11	0.12
/Primula	*Primula*	*Sphondylia*	8	8	5	5	2	0.63	0.40
/Primula	*Primula*	*Sredinskya*	1	1	1	0	0	1.00	NA
/Primula	*Primula*	*Suffrutescens*	1	1	1	1	1	1.00	1.00
/Primula	*Primula*	*Yunnanensis*	15	16	5	14	5	0.31	0.36
/Soldanella	*Soldanella*		16	16	4	0	0	0.25	NA
/Soldanella	*Bryocarpum*		1	1	1	0	0	1.00	NA
/Soldanella	*Hottonia*		2	2	2	1	1	1.00	1.00
/Soldanella	*Omphalogramma*		9	9	2	0	0	0.22	NA
Total of clade /Androsace			**153**	**155**	**66**	**1**	**1**	**0.43**	**1.00**
Total of clade /Soldanella			**28**	**28**	**9**	**1**	**1**	**0.32**	**1.00**
Total of clade /Primula			**505**	**556**	**190**	**457**	**151**	**0.34**	**0.33**
GRAND TOTAL			**690**	**738**	**265**	**459**	**153**	**0.36**	**0.33**

Notes:

1: According to the following major taxonomic works: [53] (*Androsace, Douglasia*); [54] (*Dionysia*); [55] (*Dodecatheon*); [4] (*Primula*); [56] (*Soldanella*), [5] (*Bryocarpum*, *Cortusa*, *Omphalogramma*, *Pomatosace, Primula*).

2: For the estimated number of species in *Primula*, we primarily followed Richards' monograph [4], except for Chinese species, where we followed the Flora of China [5], because Richards [4] does not accept some species shown by Yan et al. [3] to represent distinct lineages (e.g. *Primula wangii*). The true number of *Primula* species is unknown and may lay somewhere in between Hu & Kelso's and Richards' estimates. Additionally, estimates include the following recently described species: *Androsace komovensis* Schönsw. & Schneew. in: Taxon 58(2): 547 (544-549; figs.) (2009) (Section *Aretia*); *Androsace kuczerovii* Knjaz. in: Bot. Zhurn. (Moscow & Leningrad) 83(3): 137 (1998) (probably Section *Chamaejasme*, but not certain); *Primula bukukunica* Kovt. in: Bot. Zhurn. (Moscow & Leningrad) 94(12): 1836 (1835-1841; fig. 1-2) (2009) (Section *Aleuritia*); *Primula calyptrata* X.Gong & R.C.Fang in: Novon 13(2): 193 (2003) (Section *Carolinella*); *Primula arunachalensis* S.K.Basak & Maiti in: Acta Phytotax. Geobot. 51(1): 11 (2000) (Section *Chartacea*) *Primula fenghwaiana* C.M.Hu & G.Hao in: Edinburgh J. Bot. 68(2): 298 (-299; fig. 1) (2011) (Section *Chartacea*); *Primula nghialoensis* D.W.H.Rankin in: Curtis's Bot. Mag. 27(2): 138 (132-139; figs. 1-2, pl. 674) (2010) (Section *Chartacea*); *Primula rebeccae* A.J.Richards in: Plantsman n.s., 3(1): 54 (-56; fig.) (2004) (Section *Cordifoliae*); *Primula pskemensis* Lazkov in: Novosti Sist. Vyssh. Rast. 36: 36 (35-38; fig. 4) (2004) (Section *Cortusoides*); *Primula lilacina* A.J.Richards in: Plantsman n.s., 7(2): 123 (-124; fig.) (2008) (Section Muscarioides); Primula bergenioides C.M.Hu & Y.Y.Geng in: Novon 13(2): 196 (2003) (Section *Petiolares*); *Primula lihengiana* C.M.Hu & R.Li in: Ann. Bot. Fenn. 46(2): 130 (-132; fig. 1) (2009) (Section *Petiolares*); *Primula tenuituba* C.M.Hu & Y.Y.Geng in: Novon 13(2): 199 (2003) (Section *Petiolares*).

3: Breeding system information follows taxonomic literature; conflict between Richards' monograph [4] and the Flora of China [5] was judged based on discussions by Ernst [6], if possible. The fraction of all species in *Primula* that are heterostylous was calculated among species of which the breeding system is known. For this table, species that were heterostylous in some but not all populations were counted as 50% heterostylous and 50% non-heterostylous.

4: Scored according to coding scheme 3, that is, species for which heterostyly occurs in some, but not in all populations are not considered heterostylous.

Table S5. GenBank accession numbers for DNA sequence data of the 21 taxa in the Ericales chloroplast DNA dataset that was used to provide a legacy calibration for the Primulaceae dataset. This dataset is a subset of the dataset used by Bremer et al. [27] to date the orders and families of Asterids, but additionally includes *Androsace*, to be able to date the crown age of Primulaceae s.str., i.e. the most recent common ancestor of *Primula* and *Androsace*.

Taxon	*rbc*L gene	*ndh*F gene	*mat*K gene	*trn*V intron	*rps*16 intron	*trn*L intron
Fouquieriaceae *Fouquieria*	L11675	AJ236249	AJ429285	AJ429643	AJ430998	AJ430876
Polemoniaceae *Polemonium*	L11687	AF421070	AJ429292	AJ429649	AJ431004	AJ430882
Lecythidaceae *Barringtionia*	Z80174	AF421044	AJ429286	AJ429644	AJ430999	AJ430877
Ebenaceae *Diospyros*	Z80185	AF130213	AJ430197	AJ429642	AJ430996	AJ430874
Sapotaceae *Manilkara*	L01932	AF213732	AJ429295	AJ429652	AJ431007	AJ430885
Theophrastaceae *Theophrasta*	U96649	AF213762	AJ429307	AJ429663	AJ431018	AJ430895
Myrsinaceae *Myrsina*	U96652	AF213751	AJ429290	AJ429647	AJ431002	AJ430880
Primulaceae *Androsace*	AF395004	AF421114	DQ378429	N/A	FJ786608	AY274947
Primulaceae *Primula*	U96657	AF213757	AJ429293	AJ429650	AJ431005	AJ430883
Pentaphylacaceae *Pentaphylax*	AJ428891	AJ429106	AJ429291	AJ429648	AJ431003	AJ430881
Sladeniaceae *Sladenia*	AJ403004	AF421081	AJ429297	AJ429654	AJ431009	AJ430081
Ternstroemiaceae *Ternstroemia*	Z80211	AF421076	AJ429302	AJ429659	AJ431013	AJ430890
Actinidiaceae *Actinidia*	L01882	AJ236238	AJ429279	AJ429640	AJ430992	AJ430869
Roridulaceae *Roridula*	L01950	AJ236270	AJ429294	AJ429651	AJ431006	AJ430884
Clethraceae *Clethra*	L12609	AJ236242	AJ429281	AJ429526	AJ430994	AJ430871
Cyrillaceae *Cyrilla*	L01900	AF421051	AJ429282	AJ429527	AJ430995	AJ430872
Theaceae *Camellia*	L12602	AF130216	AJ429305	AJ429661	AJ431016	AJ430893
Theaceae *Schima*	Z80208	AF421073	AJ429306	AJ429662	AJ431017	AJ430894
Symplocaceae *Symplocos*	Z80192	AF421074	AJ429301	AJ429658	AJ431012	AJ430889
Styracaceae *Halesia*	Z80190	AF130214	AJ429298	AJ429655	AJ431010	AJ430082
Styracaceae *Styrax*	L12623	AF130215	AJ429300	AJ429657	AJ431011	AJ430888

Table S6. Taxa included in the Primulaceae dataset, indicating GenBank accession numbers for the four cpDNA regions included (i.e., *mat*K, *rpl*16, *trn*L, *trn*L-*trn*F), presence of heterostyly ("present", when all reports indicate heterostyly, "absent" when no reports of heterostyly exist, "both" when reports exist indicating both presence and absence of heterostyly, and "special" for atypical heterostyly; see Text S1 and notes).

Taxon	*matK*	*rpl16*	*trnL*	*trnL-trnF*	*Heterostyly present?*
Androsace adfinis	KF907831	KF907904	AY275008	AY275008	absent
Androsace albana	KF907873	KF907905	EU655583	EU655583	absent
Androsace alpina	KF907856	KF907906	AY274975	AY274975	absent
Androsace armeniaca	KF907874	KF907907	KF907977	KF907977	absent
Androsace axillaris	KF907898	KF907908	AY274949	AY274949	absent
Androsace barbulata	KF907895	KF907909	KF907978	KF907978	absent
Androsace brevis	KF907860	KF907910	AY274963	AY274963	absent
Androsace brigantiaca	KF907833	KF907911	EU655591	EU655591	absent
Androsace bulleyana	KF907881	KF907912	KF907979	KF907979	absent
Androsace bungeana	KF907834	KF907913	KF907980	KF907980	absent
Androsace cantabrica	KF907842	KF907914	AY275009	AY275009	absent
Androsace chaixii	KF907843	KF907915	AY275003	AY275003	absent
Androsace chamaejasme	DQ378429	AF402556	AF402437	DQ378838	absent
Androsace ciliata	KF907845	KF907916	AY274982	AY274982	absent
Androsace cuscutiformis	KF907899	KF907917	KF907981	KF907981	absent
Androsace cuttingii	KF907861	KF907918	KF907982	KF907982	absent
Androsace cylindrica cylindrica	KF907836	KF907919	EU655595	EU655595	absent
Androsace cylindrica hirtella	KF907837	KF907920	EU655594	EU655594	absent
Androsace cylindrica willkommii	KF907838	KF907921	AY274987	AY274987	absent
Androsace delavayi	KF907862	KF907922	KF907983	KF907983	absent
Androsace elatior	KF907900	KF907923	KF907984	KF907984	absent
Androsace elongata breistrofferi	KF907839	KF907924	EU655585	EU655585	absent
Androsace elongata elongata	KF907840	KF907925	AY275014	AY275014	absent
Androsace erecta	KF907896	KF907926	KF907985	KF907985	absent
Androsace filiformis	KF907865	KF907927	AY274955	AY274955	absent
Androsace globifera	KF907893	KF907928	KF907986	KF907986	absent
Androsace halleri specnov	KF907847	KF907930	AY275013	AY275013	absent
Androsace halleri sstr	KF907846	KF907929	EU655587	EU655587	absent
Androsace hausmannii	KF907848	KF907931	AY274984	AY274984	absent
Androsace hedraeantha	KF907844	KF907932	KF907987	KF907987	absent
Androsace helvetica	KF907857	KF907933	AY274981	AY274981	absent
Androsace hookeriana	KF907878	KF907934	KF907988	KF907988	absent
Androsace komovensis	KF907849	KF907935	EU655596	EU655596	absent
Androsace lactea	KF907850	KF907936	AY274986	AY274986	absent
Androsace lactiflora	KF907876	KF907937	EU655582	EU655582	absent
Androsace laggeri	KF907851	KF907938	AY275012	AY275012	absent
Androsace limprichtii	KF907880	KF907939	KF907989	KF907989	absent
Androsace mariae	KF907883	KF907940	KF907990	KF907990	absent
Androsace mathildae	KF907852	KF907941	EU655598	EU655598	absent
Androsace maxima	KF907897	KF907942	AY274957	AY274957	absent
Androsace maxima torrepandoi	KF907901	KF907943	KF907991	KF907991	absent
Androsace minor	KF907884	KF907944	KF907992	KF907992	absent
Androsace nortonii	KF907892	KF907945	KF907993	KF907993	absent
Androsace obtusifolia	KF907858	KF907946	AY274971	AY274971	absent
Androsace puberula	KF907832	KF907947	AY275006	AY275006	absent
Androsace pubescens	KF907859	KF907948	AY274979	AY274979	absent
Androsace pyrenaica	KF907853	KF907949	AY274977	AY274977	absent
Androsace raddeana	KF907875	KF907950	AY274960	AY274960	absent
Androsace rioxana	KF907854	KF907951	AY275004	AY275004	absent

Androsace sempervivoides	AY647535	AF402555	AF402436	DQ378837	absent
Androsace septentrionalis	KF907872	KF907952	AY274959	AY274959	absent
Androsace spinulifera	KF907894	KF907953	KF907994	KF907994	absent
Androsace stenophylla	KF907879	KF907954	KF907995	KF907995	absent
Androsace sublanata	FJ828637	N/A	FJ794240	FJ794240	absent
Androsace triflora	KF907885	KF907955	KF907996	KF907996	absent
Androsace vandellii	KF907835	KF907956	AY274968	AY274968	absent
Androsace vitaliana	KF907841	KF907957	AY274966	AY274966	special[1]
Androsace wulfeniana	KF907855	KF907958	AY274962	AY274962	absent
Bryocarpum himalaicum	DQ378424	DQ378516	DQ378605	DQ378830	absent
Cortusa brotheri	DQ378422	DQ378513	DQ378602	DQ378827	absent
Cortusa matthiola	AY647522	AY528555	AY647667	AY647737	absent
Cortusa turkestanica	DQ378421	DQ378512	DQ378601	DQ378826	absent
Dionysia aretioides	DQ378298	DQ378434	DQ378523	DQ378703	present
Dionysia bryoides	KF907868	KF907959	KF907997	KF907997	present
Dionysia gaubae	KF907871	KF907960	KF907998	KF907998	present
Dionysia haussknechtii	KF907870	KF907961	KF907999	KF907999	present
Dionysia hissarica	DQ378299	DQ378435	DQ378524	DQ378704	present
Dionysia lindbergii	KF907882	KF907962	KF908000	KF908000	present
Dionysia lurorum	KF907869	KF907963	KF908001	KF908001	present
Dionysia revoluta	KF907867	KF907964	KF908002	KF908002	present
Dionysia tapetodes	DQ378300	DQ378436	DQ378525	DQ378705	present
Dodecatheon alpinum	AY647475	AY528520	AY647620	AY647690	absent
Dodecatheon clevelandii	AY647465	AY528510	AY647610	AY647680	absent
Dodecatheon conjugens	AY647469	AY528514	AY647614	AY647684	absent
Dodecatheon dentatum	AY647485	AY528530	AY647630	AY647700	absent
Dodecatheon frigidum	AY647471	AY528516	AY647616	AY647686	absent
Dodecatheon hendersonii	AY647462	AY528507	AY647607	AY647677	absent
Dodecatheon poeticum	AY647488	AY528533	AY647633	AY647703	absent
Dodecatheon pulchellum	AY647478	AY528523	AY647623	AY647693	absent
Douglasia arctica	KF907886	KF907965	AY274998	AY274998	absent
Douglasia beringensis	AY647536	AF402557	AY274999	AY274999	absent
Douglasia gormanii	KF907888	KF907968	AY275000	AY275000	absent
Douglasia idahoensis	KF907889	KF907969	AY275001	AY275001	absent
Douglasia laevigata	KF907891	KF907966	AY274995	AY274995	absent
Douglasia nivalis	KF907887	KF907967	AY274991	AY274991	absent
Douglasia ochotensis	KF907890	KF907970	AY274996	AY274996	absent
Hottonia inflata	DQ378428	DQ378520	DQ378609	DQ378836	absent
Hottonia palustris	AY647534	AF402554	AF402435	DQ378835	special[2]
Omphalogramma delavayi	DQ378423	DQ378514	DQ378603	DQ378828	absent
Omphalogramma souliei	AY647532	DQ378515	DQ378604	DQ378829	absent
Pomatosace filicula	DQ378431	AF402559	AF402440	DQ378841	absent
Primula advena	DQ378396	AF402525	AF402405	DQ378801	present
Primula algida	DQ378340	AF402468	AF402350	DQ378745	present
Primula aliciae	DQ378303	DQ378438	DQ378527	DQ378708	present
Primula alpicola	FJ828606	N/A	FJ794205	FJ794205	present
Primula amethystina	AY647523	AY528556	AY647668	AY647738	present
Primula angustifolia	AY647514	AF402536	AY647659	AY647729	present
Primula anvilensis	DQ378355	DQ378469	DQ378558	DQ378760	present
Primula aromatica	FJ828630	N/A	FJ794233	FJ794233	present
Primula asarifolia	DQ378405	DQ378502	DQ378591	DQ378810	present
Primula aurantiaca	DQ378378	DQ378481	DQ378570	DQ378783	present
Primula aureata	DQ378375	DQ378478	DQ378567	DQ378780	present

Primula auriculata	DQ378310	AF402462	AF402344	DQ378715	present
Primula baldschuanica	DQ378342	DQ378464	DQ378553	DQ378747	present
Primula barbicalyx	FJ828647	N/A	FJ794251	FJ794251	present
Primula bella	FJ828600	N/A	FJ794198	FJ794198	present
Primula bellidifolia	DQ378312	DQ378442	DQ378531	DQ378717	both[3]
Primula blattariformis	FJ828654	N/A	FJ794261	FJ794261	present
Primula boothii	DQ378370	DQ378475	DQ378564	DQ378775	present
Primula borealis	AY647527	AF402488	AY647672	AY647742	present
Primula boreiocalliantha	FJ828620	N/A	FJ794220	FJ794220	present
Primula bracteata	DQ378409	AF402548	AF402429	DQ378814	present
Primula bracteosa	DQ378371	DQ378476	DQ378565	DQ378776	present
Primula cachemiriana	DQ378325	DQ378452	DQ378541	DQ378730	present
Primula calderiana	DQ378374	AF402514	AF402394	DQ378779	present
Primula calliantha	DQ378397	DQ378496	DQ378585	DQ378802	present
Primula calyptrata	FJ828646	N/A	FJ794250	FJ794250	absent
Primula capillaris	AY647519	AY528554	AY647664	AY647734	present
Primula capitata	DQ378326	DQ378453	DQ378542	DQ378731	present
Primula caveana	DQ378400	DQ378498	DQ378587	DQ378805	present
Primula celsiiformis	FJ828607	N/A	FJ794206	FJ794206	present
Primula cernua	DQ378317	DQ378446	DQ378535	DQ378722	present
Primula chapaensis	FJ828645	N/A	FJ794249	FJ794249	present
Primula chionantha	DQ378387	DQ378488	DQ378577	DQ378792	present
Primula chungensis	DQ378382	DQ378484	DQ378573	DQ378787	both[4]
Primula cicutariifolia	DQ378366	DQ378471	DQ378560	DQ378771	absent
Primula clarkei	DQ378307	AF402460	AF402342	DQ378712	present
Primula clusiana	AY647490	AY528534	AY647635	AY647705	present
Primula cockburniana	DQ378380	DQ378483	DQ378572	DQ378785	absent
Primula cortusoides	DQ378412	DQ378505	DQ378594	DQ378817	present
Primula cuneifolia cuneifolia	AY647502	AY528542	AY647647	AY647717	present
Primula cuneifolia saxifragifolia	AY647506	AY528545	AY647651	AY647721	absent
Primula cusickiana cusickiana	AY647515	AY528550	AY647660	AY647730	present
Primula cusickiana maguirei	AY647516	AY528551	AY647661	AY647731	present
Primula darialica	DQ378341	AF402470	AF402352	DQ378746	present
Primula deflexa	DQ378315	DQ378444	DQ378533	DQ378720	present
Primula denticulata	DQ378323	DQ378450	DQ378539	DQ378728	present
Primula deorum	AY647497	AF402531	AY647642	AY647712	present
Primula deuteronana	DQ378372	DQ378477	DQ378566	DQ378777	present
Primula dryadifolia	DQ378406	AF402551	AF402432	DQ378811	present
Primula edelbergii	AY647528	AF402452	AY647673	AY647743	present
Primula efarinosa	FJ828616	N/A	FJ794216	FJ794216	present
Primula egaliksensis	DQ378349	AF402481	AF402363	DQ378754	absent
Primula elatior	DQ378361	AF402504	AF402384	DQ378766	present
Primula elliptica	DQ378306	AF402459	AF402341	DQ378711	present
Primula erratica	DQ378322	AF402471	AF402353	DQ378727	present
Primula excapa	DQ378367	DQ378472	DQ378561	DQ378772	present
Primula eximia	AY647525	AF402522	AY647670	AY647740	absent
Primula faberii	AY647524	AY528557	AY647669	AY647739	present
Primula farinosa	DQ378345	AF402474	AF402356	DQ378750	present
Primula fasciculata	DQ378329	DQ378455	DQ378544	DQ378734	present
Primula fedtschenkoi	DQ378399	AF402526	AF402406	DQ378804	present
Primula firmipes	DQ378360	AF402502	AF402382	DQ378765	present
Primula flaccida	DQ378318	DQ378447	DQ378536	DQ378723	present
Primula floribunda	DQ378296	AF402454	AF402336	DQ378701	both[5]
Primula florida	DQ378302	DQ378437	DQ378526	DQ378707	present
Primula forbesii	AY647520	AF402540	AY647665	AY647735	present
Primula forrestii	DQ378410	AF402549	AF402430	DQ378815	present
Primula gaubeana	DQ378297	DQ378433	DQ378522	DQ378702	present

Primula gemmifera	DQ378332	AF402495	AF402375	DQ378737	present
Primula geraniifolia	DQ378417	AF402546	AF402426	DQ378822	present
Primula glabra	DQ378331	DQ378457	DQ378546	DQ378736	present
Primula glaucescens	KF907864	KF907971	KF908003	KF908003	present
Primula glomerata	DQ378324	DQ378451	DQ378540	DQ378729	present
Primula glutinosa	AY647495	AF402533	AY647640	AY647710	present
Primula grandis	AY647531	AF402505	AY647676	AY647746	absent
Primula halleri	KF907903	KF907972	KF908004	KF908004	absent
Primula heucherifolia	DQ378415	DQ378508	DQ378597	DQ378820	present
Primula hirsuta	AY647499	AY528540	AY647644	AY647714	present
Primula hongshanensis	DQ378391	DQ378492	DQ378581	DQ378796	present
Primula incana	DQ378347	AF402478	AF402360	DQ378752	absent
Primula interjacens	FJ828610	N/A	FJ794209	FJ794209	present
Primula involucrata	DQ378328	DQ378454	DQ378543	DQ378733	present
Primula japonica	DQ378379	DQ378482	DQ378571	DQ378784	absent
Primula juliae	DQ378364	AF402508	AF402388	DQ378769	present
Primula kisoana	DQ378414	DQ378507	DQ378596	DQ378819	present
Primula latisecta	DQ378416	DQ378509	DQ378598	DQ378821	present
Primula laurentiana	DQ378348	AF402479	AF402361	DQ378753	absent
Primula littledalei	DQ378401	DQ378499	DQ378588	DQ378806	present
Primula luteola	DQ378309	AF402461	AF402343	DQ378714	present
Primula malacoides	DQ378408	AF402541	AF402421	DQ378813	present
Primula malvacea	FJ828651	N/A	FJ794257	FJ794257	present
Primula marginata	AY647492	AF402530	AY647637	AY647707	present
Primula maximowiczii	DQ378398	DQ378497	DQ378586	DQ378803	present
Primula megaseifolia	DQ378363	AF402507	AF402387	DQ378768	present
Primula membranifolia	DQ378304	AF402458	AF402340	DQ378709	present
Primula merrilliana	FJ828589	N/A	FJ794196	FJ794196	present
Primula minima	AY647494	AY528537	AY647639	AY647709	present
Primula minor	DQ378394	DQ378495	DQ378584	DQ378799	present
Primula mistassinica	DQ378352	AF402485	AF402367	DQ378757	present
Primula modesta	DQ378357	AF402490	AF402371	DQ378762	present
Primula mollis	DQ378418	AF402547	AF402427	DQ378823	both[6]
Primula moupinensis	FJ828614	N/A	FJ794214	FJ794214	present
Primula muscarioides	DQ378311	DQ378441	DQ378530	DQ378716	present
Primula muscoides	DQ378337	DQ378461	DQ378550	DQ378742	absent
Primula nipponica	AY647508	AY528546	AY647653	AY647723	present
Primula nivalis	DQ378390	DQ378490	DQ378579	DQ378794	present
Primula nutans	AY647526	AF402494	AY647671	AY647741	present
Primula obconica	DQ378403	AF402542	AF402422	DQ378808	both[7]
Primula odontocalyx	DQ378368	DQ378473	DQ378562	DQ378773	present
Primula orbicularis	DQ378388	DQ378489	DQ378578	DQ378793	present
Primula ovalifolia	FJ828605	N/A	FJ794204	FJ794204	present
Primula palinuri	AY647489	AF402532	AY647634	AY647704	present
Primula parryi	AY647512	AY528548	AY647657	AY647727	present
Primula partschiana	FJ828593	N/A	FJ794190	FJ794190	present
Primula petelotii	DQ378369	DQ378474	DQ378563	DQ378774	present
Primula pinnata	DQ378344	DQ378466	DQ378555	DQ378749	present
Primula pinnatifida	DQ378316	DQ378445	DQ378534	DQ378721	present
Primula poissonii	FJ828619	N/A	FJ794219	FJ794219	present
Primula polyneura	FJ828627	N/A	FJ794227	FJ794227	present
Primula prenantha	DQ378383	AF402519	AF402399	DQ378788	absent
Primula primulina	DQ378335	DQ378460	DQ378549	DQ378740	present
Primula prolifera	DQ378384	DQ378485	DQ378574	DQ378789	both[8]
Primula pulchella	DQ378339	DQ378463	DQ378552	DQ378744	present
Primula pulverulenta	DQ378385	DQ378486	DQ378575	DQ378790	present
Primula pumilio	DQ378327	AF402493	AF402373	DQ378732	present
Primula pycnoloba	FJ828612	N/A	FJ794212	FJ794212	present

Primula reidii	DQ378320	AF402467	AF402349	DQ378725	present
Primula reptans	DQ378336	AF402496	AF402376	DQ378741	present
Primula reticulata	DQ378358	DQ378470	DQ378559	DQ378763	present
Primula rotundifolia	DQ378402	DQ378500	DQ378589	DQ378807	present
Primula rugosa	FJ828644	N/A	FJ794248	FJ794248	present
Primula rupestris	FJ828585	N/A	FJ794182	FJ794182	present
Primula rusbyi	AY647513	AY528549	AY647658	AY647728	present
Primula saturata	FJ828650	N/A	FJ794256	FJ794256	present
Primula scandinavica	DQ378351	AF402483	AF402365	DQ378756	absent
Primula scotica	KF907902	KF907973	KF908005	KF908005	absent
Primula secundiflora	FJ828613	N/A	FJ794213	FJ794213	present
Primula septemloba	FJ828656	N/A	FJ794263	FJ794263	absent
Primula serrata	DQ378343	DQ378465	DQ378554	DQ378748	present
Primula serratifolia	FJ828617	N/A	FJ828589	FJ828589	present
Primula sertulum	FJ828604	N/A	FJ794203	FJ794203	present
Primula siamensis	DQ378319	DQ378448	DQ378537	DQ378724	present[9]
Primula simensis	DQ378295	DQ378432	DQ378521	DQ378700	absent
Primula sinensis	FJ828584	N/A	FJ794181	FJ794181	present
Primula sinolisteri	DQ378404	DQ378501	DQ378590	DQ378809	both[10]
Primula sinomollis	FJ828634	N/A	FJ794237	FJ794237	present
Primula sonchifolia	DQ378373	AF402513	AF402393	DQ378778	present
Primula soongii	DQ378393	DQ378494	DQ378583	DQ378798	present
Primula souliei	DQ378305	DQ378439	DQ378528	DQ378710	present
Primula specuicola	DQ378354	AF402487	AF402368	DQ378759	present
Primula stirtoniana	DQ378334	DQ378459	DQ378548	DQ378739	present
Primula stuartii	DQ378392	DQ378493	DQ378582	DQ378797	present
Primula suffrutescens	AY647510	AY528547	AY647655	AY647725	present
Primula tanneri nepalensis	DQ378376	DQ378479	DQ378568	DQ378781	present
Primula tanneri tsariensis	DQ378377	DQ378480	DQ378569	DQ378782	present
Primula tenuiloba	DQ378338	DQ378462	DQ378551	DQ378743	present
Primula tosaensis	DQ378411	DQ378504	DQ378593	DQ378816	present
Primula tschuktshorum	DQ378395	AF402523	AF402403	DQ378800	present
Primula veris	AY647530	AF402503	AY647675	AY647745	present
Primula verticillata	DQ378294	AF402453	AF402335	DQ378699	absent
Primula vialii	DQ378313	AF402466	AF402348	DQ378718	present
Primula villosa	KF907863	KF907974	KF908006	KF908006	present
Primula violaceae	KF907866	KF907975	KF908007	KF908009	present
Primula walshii	KF907877	KF907976	KF908008	KF908010	present
Primula waltonii	DQ378359	AF402500	AF402380	DQ378764	present
Primula wangii	FJ828648	N/A	FJ794252	FJ794252	present
Primula warshenewskiana	DQ378308	DQ378440	DQ378529	DQ378713	present
Primula watsonii	DQ378314	DQ378443	DQ378532	DQ378719	both[11]
Primula wigramiana	DQ378321	DQ378449	DQ378538	DQ378726	present
Primula yunnanensis	DQ378301	AF402457	AF402339	DQ378706	present
Soldanella alpina	DQ378425	DQ378517	DQ378606	DQ378832	absent
Soldanella minima	DQ378426	DQ378518	DQ378607	DQ378833	absent
Soldanella pusilla	AY647533	AF402553	AF402434	DQ378831	absent
Soldanella villosa	DQ378427	DQ378519	DQ378608	DQ378834	absent

Notes:

1: Schaeppi [31] documented atypical heterostyly (see text S1), with strong stylar but weak anther polymorphism.

2: The short-style morphs of *Hottonia palustris* have anthers positioned well above the corolla, with filaments that are partially free, whereas other heterostylous species have a narrow floral tube to which filaments are fused, concealing sexual organs within [30].

3: Among 46 investigated plants Ernst ([6]: 78) observed plants with and without heterostyly, but the majority (26) could not be unambiguously assigned to either one, because sexual organ positions appear to be extremely variable in this species, also among plants that seem heterostylous at first

glance. Hence, this species does not display clear heterostyly in most populations and was therefore coded as non-heterostylous in scheme 2.

4: Ernst ([57]: 140-149) showed that populations of this species can be heterostylous, non-heterostylous or consist of a mixture of either floral morph and a non-heterostylous form. Scoring under scheme 2 is thus as non-heterostylous.

5: Ernst ([6]: 71) investigated 165 plants in the herbaria Edinburgh, Kew, and Calcutta, and of the 147 plants that had well-preserved flowers, 138 clearly displayed heterostyly. Scoring in scheme 2 is therefore heterostylous.

6: According to Ernst ([58]: 74-78) heterostyly is absent in most of the herbarium material of this species; those few collections showing heterostyly also differ in other characters from the non-heterostylous material, which suggests that the heterostylous material may actually represent a different species. Therefore, scoring under scheme 2 is as non- heterostylous.

7: Ernst ([6]: 82) classifies this species as heterostylous, in which only occasionally aberrant forms occur, as of 120 investigated flowers, only 2 lacked heterostyly. Hence, scoring under scheme 2 is as heterostylous.

8: *P. prolifera* has an extremely complex taxonomic history and has a remarkably disjunct distribution, with heterostylous populations in the Eastern Himalaya, and non-heterostylous populations in high mountains on Java and Sumatra (Indonesia) as well as peninsular Malaysia ([4], [59]:189-191). There are no accounts of populations in the Himalaya that lack heterostyly, nor has heterostyly been reported from Malaysia or Indonesia. Scoring in scheme 2 is as heterostylous, because the sampled material in this study comes from the Himalaya, and the complex taxonomic history may suggest that disjunct material is distantly related.

9: Richards [4] states the species is identical to *P. spicata* except in leaf characters; *P. spicata* differs only in habit and flower colour from *P. flaccida*; *P. flaccida* is claimed to be heterostylous. Not discussed by Ernst [6].

10: Ernst [6] classifies this species as heterostylous but ignores *var. aspera* which lacks heterostyly according to Richards [4]. Because the material used in our study does not represent *var. aspera*, the species was scored as heterostylous in character coding scheme 2.

11: Ernst ([6]: 80) states that 9 of 11 investigated herbarium sheets contained 36 plants with heterostyly; 2 herbarium sheets contained mixtures of heterostylous morphs and plants that lacked heterostyly. The species was scored as non-heterostylous in character coding scheme 2, because heterostyly appears to be rare in this species.